Turkish Journal of Earth Sciences (Turkish J. Earth Sci.), Vol. 20, 2011, pp. 27–56. Copyright ©TÜBİTAK
doi:10.3906/yer-1001-30 First published online 23 June 2010

Stratigraphy, Sedimentology and Palynology of the Neogene–Pleistocene(?) Rocks Around Akçaşehir-Tire-İzmir (Küçük Menderes Graben, Western Anatolia)

TAHİR EMRE[1], METİN TAVLAN[2], MEHMET SERKAN AKKİRAZ[3] & İSMAİL İŞİNTEK[1]

[1] Dokuz Eylül Üniversitesi, Jeoloji Mühendisliği Bölümü, Tınaztepe Yerleşkesi, Buca, TR–35160 İzmir, Türkiye (E-mail: tahir.emre@deu.edu.tr)

[2] Sardes Nikel Madencilik A.Ş., Akdeniz Caddesi, No: 14, Birsel İş Merkezi D: 502, Pasaport, Konak, TR–35210 İzmir, Türkiye

[3] Dumlupınar Üniversitesi, Mühendislik Fakültesi, Jeoloji Mühendisliği Bölümü, Merkez Kampüsü, Tavşanlı Yolu 10. km, TR–43100 Kütahya, Türkiye

Received 23 January 2010; revised typescript receipt 04 June 2010; accepted 23 June 2010

Abstract: The basement rocks located in the central part of the southern edge of the Küçük Menderes Graben, around Akçaşehir-Tire are composed of marbles, schists, gneisses and metagabbros of the Ödemiş–Kiraz submassif of the Menderes Massif, and schists, marbles and meta-olistostromes of the Cycladic Complex. The basement is unconformably overlain by Neogene–Quaternary continental sediments. These continental basin fills are comprised of the Ayaklıkırı Formation, the Aydoğdu Formation and alluvium that unconformably overlies them. The Lower–Upper Miocene Ayaklıkırı Formation consists of lacustrine and fluvial deposits. The Plio–Pleistocene (?) Aydoğdu Formation is made up of alluvial fan deposits. Vast plains of alluvium cover the youngest formations.

The lowest part of the Ayaklıkırı Formation is represented by terrestrial to very shallow lake environments, represented by silts, clays, laminated micritic carbonates, ostracod-bearing laminated algal, microbial and peloidal microbial carbonates, algal carbonate crusts and pebbly, sandy, clayey, micritic carbonates.

Palynological data collected from coal beds around Akçaşehir-Tire shows that the Ayaklıkırı Formation was deposited during the latest Early Miocene–earliest Late Miocene. Palynological data and some gastropoda taxa such as *Planorbis* sp. and *Limnea* sp. indicate that the Ayaklıkırı Formation was deposited in a lacustrine environment. Palaeoclimatic results indicate a warm temperate to humid climate preceding the Middle Miocene Climatic Optimum.

Key Words: Western Anatolia, Küçük Menderes Graben, Neogene–Quaternary terrestrial sediment, Akçaşehir coal, palynology, continental carbonate

Akçaşehir-Tire-İzmir Çevresindeki Neojen–Pleyistosen(?) Yaşlı Kayaçların Stratigrafisi, Sedimentolojisi ve Palinolojisi (Küçük Menderes Grabeni, Batı Anadolu)

Özet: Küçük Menderes Grabeni'nin güney kenarının orta kesiminde yer alan Akçaşehir-Tire dolaylarında, Menderes Masifi Ödemiş-Kiraz asmasifi'nin mermer, şist, gnays ve metagabroları ve Kikladik Kompleks'in şişt, mermer ve metaolistromları temeli oluşturur. Temel kayaları, Neojen–Kuvaterner yaşlı karasal tortullar açısal uyumsuz olarak üzerler. Bu tortullar, birbirlerini açısal uyumsuzlukla üzerleyen, en geç Erken Miyosen–en erken Geç Miyosen yaşlı Ayaklıkırı Formasyonu, Pliyo–Pleyistosen(?) yaşlı Aydoğdu Formasyonu ve Holosen yaşlı alüvyonlardır. Ayaklıkırı Formasyonu göl ve akarsu çökellerinden, Aydoğdu Formasyonu alüvyon yelpazesi çökellerinden oluşur. En genç çöküntü alanlarını dolduran alüvyonlar geniş düzlükleri kaplarlar.

Ayaklıkırı Formasyonu en alt bölümü karasaldan çok sığ göl ortamına değişen bir ortamda çökelen, siltli, killi laminalı mikritik karbonatlar, ostrakodlu, laminalı mikrobiyal ve peloidal mikrobiyal karbonatlar, algal karbonat kabuklar ve çakıllı, kumlu, killi mikritik karbonat düzeyleriyle temsil edilir.

Akçaşehir çevresinde, Ayaklıkırı Formasyonu'nun içerdiği kömür düzeylerinden elde edilen palinolojik veriler, Ayaklıkırı Formasyonu'nun en geç Erken Miyosen–en erken Geç Miyosen süresince çökeldiğini belirtmektedir. Palinolojik veriler ve *Planorbis* sp., *Limnea* sp. gasropodları Ayaklıkırı Formasyonu'nun kömürlü düzeylerinin gölsel bir ortamda çökelmiş olduğunu belirtir. Paleoiklimsel sonuçlar, küresel ölçekte Orta Miyosen iklimsel maksimumundan önceki nemli sıcak bir iklimi tanımlamaktadır.

Anahtar Sözcükler: Batı Anadolu, Küçük Menderes Grabeni, Neojen–Kuvaterner karasal tortul, Akçaşehir kömürü, palinoloji, karasal karbonatlar

Introduction

The geological study of the Menderes graben began in the nineteenth century (Hamilton & Strickland 1840; Tchihatcheff 1869; Phillipson 1911, 1918), although the total number of studies focused on the structure of the Küçük Menderes Graben are relatively few (Philippson 1910–1915, 1918; Erinç 1955; Ketin 1968; McKenzie 1978; Dewey & Şengör 1979; Dumont *et al.* 1979; Angelier *et al.* 1981; Şengör 1982, 1987; Jackson & McKenzie 1984; Şengör *et al.* 1984, 1985; Rojay *et al.* 2001, 2005; Emre *et al.* 2003; Bozkurt & Rojay 2005; Emre & Sözbilir 2007).

Previous researchers showed that the E–W-striking Küçük Menderes valley was part of an E–W- and WNW–ESE-trending graben structure started to develop in the Neogene with N–S extension (Philipson 1910–1915, 1918; Ketin 1968; McKenzie 1978; Jackson & McKenzie 1984; Şengör *et al.* 1984; Şengör 1987).

A north-dipping fault has been clearly observed along western parts of the southern margin (Erinç 1955; Şengör *et al.* 1985). In the west, this fault passes through the NE of Ephesus (Dumont *et al.* 1979; Angelier *et al.* 1981), and extends to the Aegean Sea. According to Rojay *et al.* (2001, 2005), the Küçük Menderes Graben, trending from Beydağ to Belevi developed over an E–W-trending syncline. Seyitoğlu & Işık (2009) suggested a huge regional syncline which developed by further exhumation of the central Menderes Massif, along with the rolling hinges of faults bounding the Alaşehir and Büyük Menderes grabens. In the area a pre-Early Pliocene N–S-trending compressional phase occurred between the extensional phases that produced low- and high-angle normal faults (Bozkurt & Rojay 2005).

There are several studies concerning the Neogene sediments outcropping in the Küçük Menderes Graben (Ozansoy 1960; Nakoman 1971; United Nations 1974; Kaya 1987; Gemici *et al.* 1992; Ercan *et al.* 1996; Rojay *et al.* 2001; Emre *et al.* 2003; Bozkurt & Rojay 2005; Emre *et al.* 2005, 2006b; Emre & Sözbilir 2005; Rojay *et al.* 2005).

The Küçük Menderes Graben contains sub-basins, which developed during the Neogene–Quaternary period. Miocene–Quaternary sediments were deposited in the Kiraz, Dağkızılca-Torbalı and Selçuk sub-basin. Quaternary sediments also accumulated in the Ödemiş and Bayındır sub-basins (Rojay *et al.* 2001, 2005).

Recent discoveries about both the stratigraphy and ages of the Neogene–Quaternary successions by several researchers are contradictory (Bozkurt & Rojay 2005; Emre & Sözbilir 2005; Rojay *et al.* 2005; Emre *et al.* 2006b).

Emre & Sözbilir (2005) determined the age of the Başova Andesites that crop out to the NE, E and SE of Kiraz town to be 14.7±0.1 – 14.3±0.1 Ma ($^{40}Ar/^{39}Ar$), while Emre *et al.* (2006), recorded that the latest Middle Miocene–late Miocene Suludere Formation, dated by ostracod faunal assemblages, unconformably overlies metamorphic rocks and the Middle Miocene Başova Andesites. The Plio–Pleistocene Aydoğdu Formation is formed of alluvial fan deposits that accumulated under the control of high-angle faults. This unit unconformably overlies the Suludere Formation, which was deposited in lacustrine and fluvial environments. Emre & Sözbilir (2007) indicated that the Kiraz sub-basin was formed in two phases: a late Middle Miocene–Late Miocene compression-uplift regime is overprinted by the block faulting stage of the extensional neotectonic regime initiated in the Plio–Pleistocene which continues to the present day. Compression and extension stress is accommodated by NE–SW-trending strike-slip fault systems. The first phase, comprising thrust and strike-slip faults associated with uplift in the northern side of the basin and the deformation indicating N–S compression, has only been observed in the northern margin of the basin. The subsequent extensional tectonic regime is represented by the normal fault system located on opposite sides of the basin.

Additionally, several studies have been undertaken which attempt to date the Neogene sediments outcropping in the Tire area. Ozansoy (1960) considered that the sediments cropping out in the Tire area were deposited in the Burdigalian (end of the Lower Miocene), based on the presence of *Dinotherium naricum* and *Serridentinus subtapiroidem*. Additionally, Becker-Planten (1975) found *Dinotherium, Gomphotherium, Anchitherium* and *Rhinocerotidae* in the İzmir-Tire-Torbalı Neogene sediments and dated the lignites as late Burdigalian (late Aragonian). Özcan (1984) studied 60 palynological samples from the Tire area and indicated that the relative percentages of spore and pollen species are low. Kaya (1987) described *Anchitherium aurelianense* and *Aceratherium tetradoctylum* and interpreted the age of Tire lignites as early Middle Miocene, taking regional expansion of the species into consideration. Gemici *et al.* (1992) studied the macro and microfloras of the Akçaşehir-Tire lignites and dated the sediments as Middle Miocene on the basis of limited palynological and palaeobotanical findings.

In this study, the Neogene–Quaternary sediments have been differentiated and dated by means of palynological data. Additionally, detailed stratigraphical, sedimentological and palynological aspects of the sedimentary infill of the Akçaşehir (Tire) basin located at the southern margin of the Küçük Menderes Graben are described here for the first time (Figure 1).

Stratigraphy

The basement of the study area consists of Precambrian to Eocene (Candan *et al.* 2001; Özer *et al.* 2001) rocks. The units are composed of schists, marbles, orthogneiss, paragneiss and metagabbros of the Ödemiş-Kiraz Sub-massif of the Menderes Massif and schist, together with marble and meta-olistostroms of the Cycladic Complex (Candan *et al.* 1997, 2007; Çetinkaplan 2002). These units are covered by sedimentary rocks of the latest Early Miocene–earliest Late Miocene Ayaklıkırı Formation, the Plio–Pleistocene(?) Aydoğdu Formation, and Recent alluvium (Figure 2). The Ayaklıkırı Formation is unconformably overlain by the Aydoğdu Formation and alluvium.

Ayaklıkırı Formation

The unit crops out over a total area of 22 km^2 around Ayaklıkırı and Akçaşehir villages (Figure 3). The formation is first described in this study and named after Ayaklıkırı village where the best exposures are located. The formation consists of generally beige, grey and milky brown, lacustrine and fluvial sedimentary rocks with distinct coal seams.

Description of Lithofacies– Conglomerates are generally beige, grey and sporadically reddish brown and medium to thick bedded. The degree of lithification varies between poorly and very well lithified. These sediments are generally moderately mature and range from poorly to well sorted. Sometimes normal or reverse grading is present. Conglomerate occasionally grades into gravelly sandstones which can in turn pass into medium–coarse-grained sandstones. Clasts are often angular with jagged edges or may be moderately rounded or somewhat angular or platy. They are rarely well-rounded gravels with low to mid sphericity. Gravels have a ratio of between 20–90 %, and their sizes vary from a few millimetres across to large boulders (rarely 70 x 45 x 35 cm). Nearly all clasts were derived from metamorphic rocks or meta-olistostromes. The dominant gravel type and amount varies according to the location of the sediment source. In some places, they may be composed of 60–90% marble, 10–30% of schist and of minor quartzite or 60% of schist, 20–30% of marble, in others 60–90% of gneiss and remaining schist and metaquartzite, or sometimes 45% of schist and 50% of gneiss, in some areas 80% of meta-ophiolite and 20% of metaquartzite. Conglomerates which are grain-supported generally have fine–medium sand, silt, coarse sand, granule and locally a clay-sand

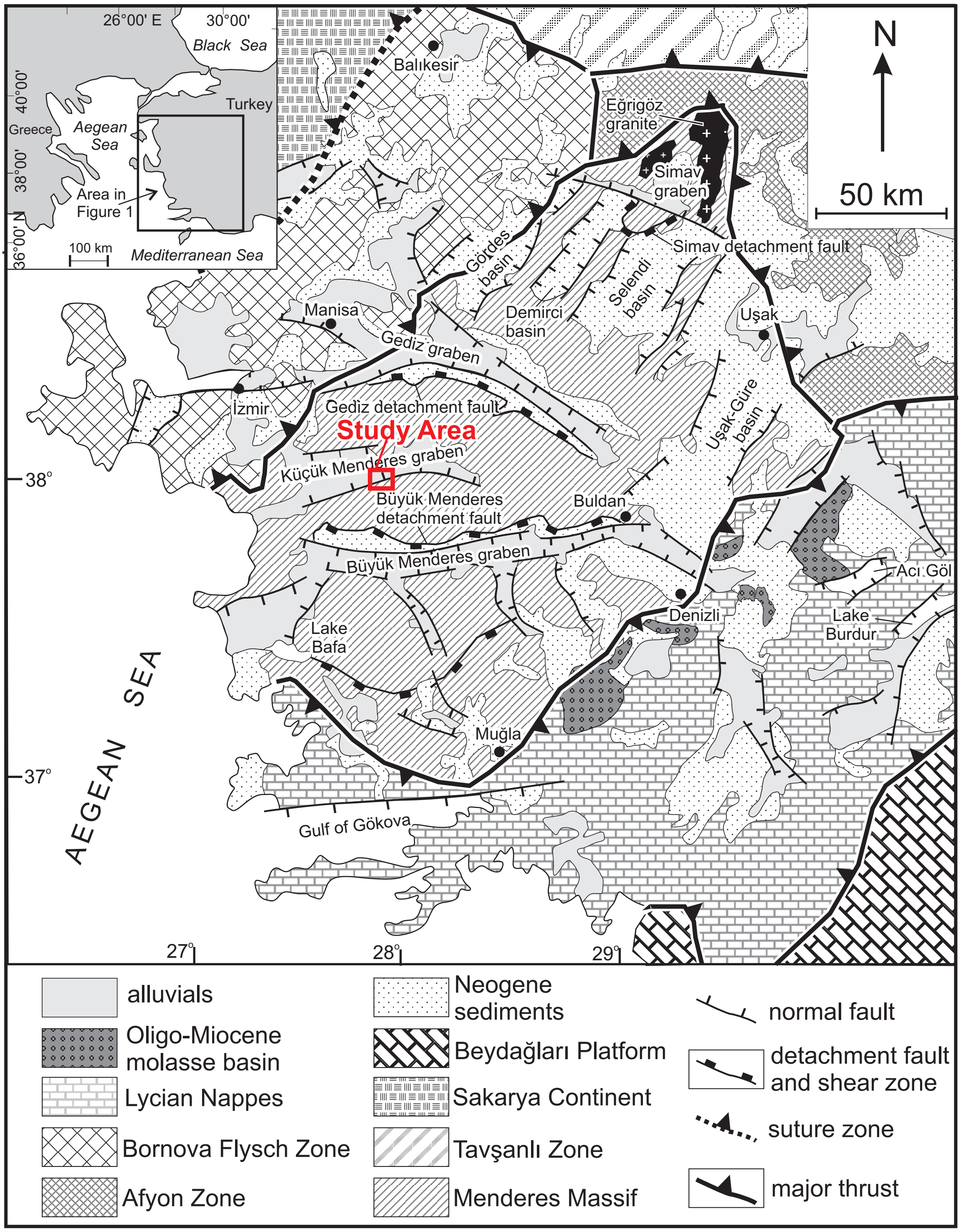

Figure 1. Regional tectonostratigraphic location of the study area (modified from Sözbilir 2005).

matrix, or are carbonate cemented. In the lower parts of the succession, the cement is composed of algal limestone or of marls. Frequently, matrix or cement is grey, beige and pink. Conglomerates have some thin interlayers and lenses of sandstone. The succession displays variation in lithification and

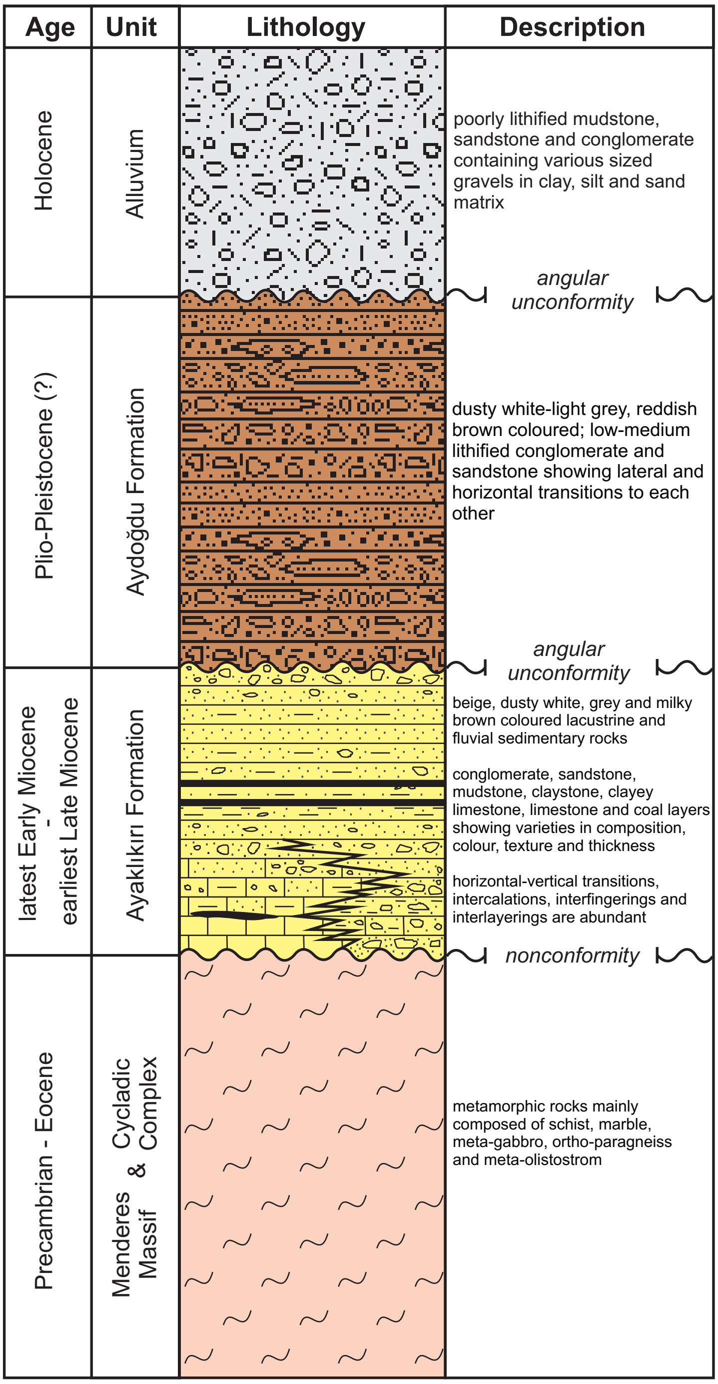

Figure 2. Generalized columnar stratigraphic section of the study area.

sorting properties, but overall it is poorly sorted and generally poorly lithified. Long axes of gravels or large surfaces of platy gravels are generally parallel to stratification.

Gravelly sandstone and gravelly mudstone have a gradational contact with the conglomerates and often have conglomerate and sandstone intercalated with them. This lithofacies is light brick red, milky

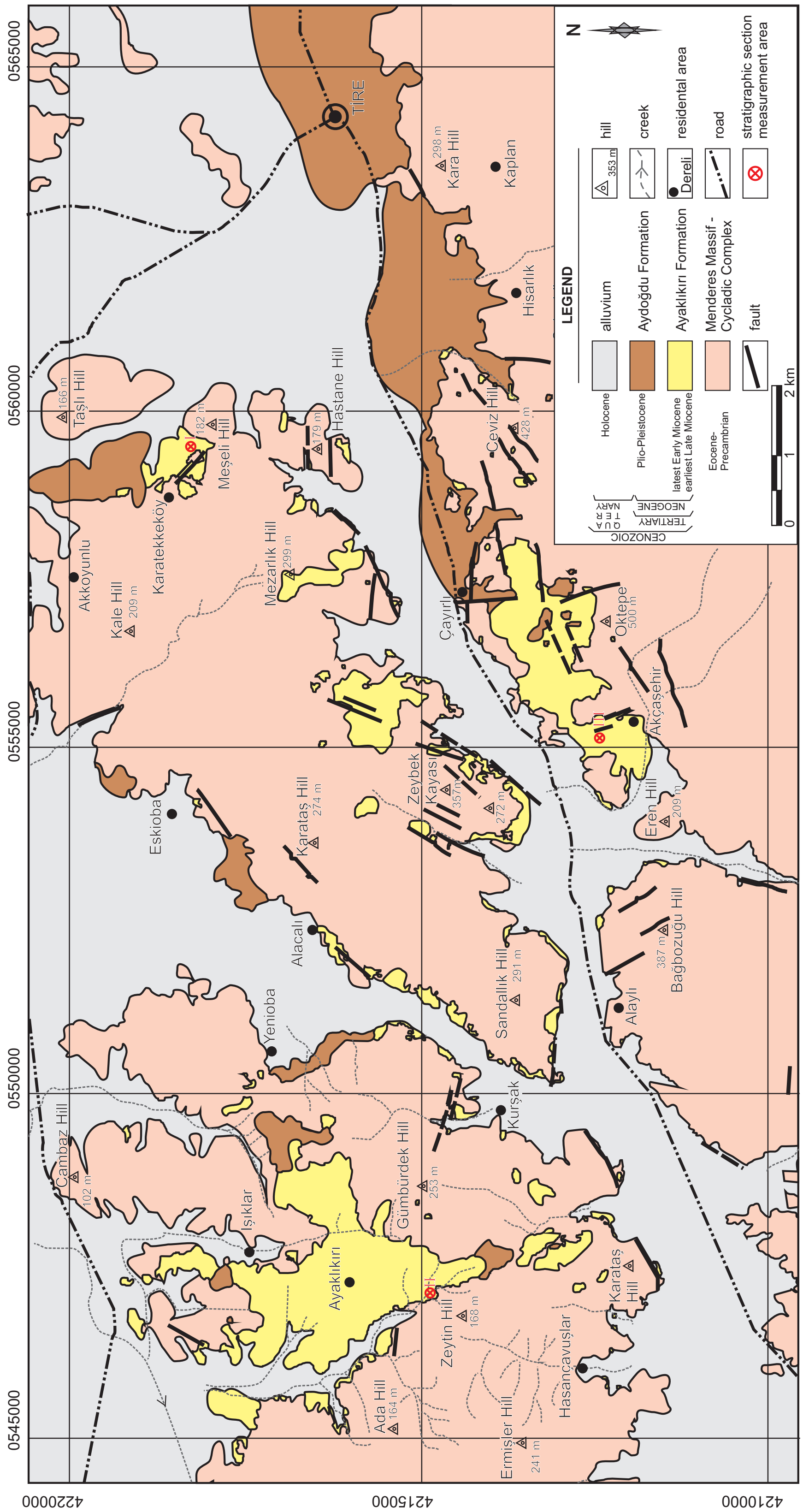

Figure 3. Simplified geological map of the Akçaşehir-Tire-İzmir area

brown and grey, variably lithified and with medium thick bedding. The proportion of scattered gravels with grains smaller than 3 cm is less than 10% within medium-coarse-grained sandstones or siltstone. In some gravelly mudstone levels, there are some single channel fills, with scraping and load casts. Channel fills which cut down through different beds are 5–6 m wide. These conglomerates are grey, poorly lithified and coarse grained (max: 25–30 cm), they are very poorly sorted with clasts mostly derived from schist and quartzite.

Sandstones are generally, grey and beige; locally greenish grey to orange-yellow. They are generally, poorly but in some cases are well lithified, frequently fine–coarse grained, mid-thick but occasionally thin-bedded or laminated. In some places, gravels contain mica flakes derived from basement rock. Plate and rod shaped, dark coloured plant relics are aligned parallel to the stratification of laminated sandstone. Sandstones rarely display cross-stratification and contain bird's eye voids and white carbonate nodules. The layers are generally regular in grain size, but graded bedding is sometimes present. Occasionally, coarse-grained gravelly sandstones at the base grade upward to fine-grained, carbonate cemented sandstones and some mudstones, claystones, fine gravelly sandstones or marls. The sandstones intercalated with coal, mudstone or conglomerates, include lenses and interbeds of conglomerate, gravelly sandstone, mudstone, claystone, clayey limestone or limestone. These lenses or interlayers have very thin or thin bedding.

Claystones and mudstones are generally, milky brown, some are greenish grey and beige. They are generally, poorly lithified, medium to thin bedded, but some are thick or very thin bedded or laminated. Shales and mudstones are frequently found intercalated with each other and more rarely with limestone, marl, coal or sandstones. In some places, they incorporate conglomerate, sandstone, gravelly claystone/mudstone, clayey limestone or limestone lenses or interlayers, or pass laterally into these lithologies. The thickness of these lenses or interlayers ranges between 15 and 20 cm. Claystones and mudstones contain rare gastropod fossils, irregularly shaped calcareous nodules or scattered pebbles. The nodules have a porous structure and are white. They have a maximum size of 2–3 cm and form up to 2–3% of the bed. The proportion of scattered gravels (rarely up to 7–8 cm) in the claystones and mudstones, derived from schist, marble and quartzite is less than 5%.

Limestones include beige, pinky red and light grey thin–medium-bedded, although rarely very thin or thick-bedded, algal limestones, and clayey or sandy limestones. Limestones are found intercalated with mudstone or coal and have a spotted appearance, manganese dendrites and are silicified in some parts. Algal limestones, comprising superposed semi-spherical stromatolites, are usually located at the base of the succession and pass laterally and horizontally into clayey or gravelly limestones or mudstone or sandstone or conglomerate. The cement of these conglomerates located at the base of the succession is mainly made of algal limestone. Poorly lithified clayey limestones (marls) with a bitumen smell contain rare amorphous carbonate nodules, 1–2 mm sized bird's eye voids, plant spikes, gastropod fossils and a minor percentage (1%) of schist pebbles and granules smaller than 7 mm.

1250 m south of Ayaklıkırı (Figure 3), conglomerates and mudstones dominate the succession (Figure 4). Gravels generally have a clay or sand matrix and some are cemented with marl. Mudstones contain conglomerate lenses in patches and can be intercalated with the sandstones. Conglomerates display transition to sandstones or carbonated sandstones containing pebbles and granules. Carbonated sandstones display transition to mudstones.

750 m southeast of Karatekkeköy (Figure 3), the succession is dominantly formed from conglomerates (Figure 5). The carbonate cemented conglomerates at the base, display a sharp transition into gravelly sandstone and gravelly mudstone above. Eroded channel fills are found in the gravelly mudstone horizons.

Coal seams are intercalated with claystones, limestones and sandstones in the succession. These coal seams are mined 500 m north of Akçaşehir village. Coal-bearing successions are named by their coal seam thickness as large, medium and small vein. Total thicknesses of the layered coals reach 385 cm in

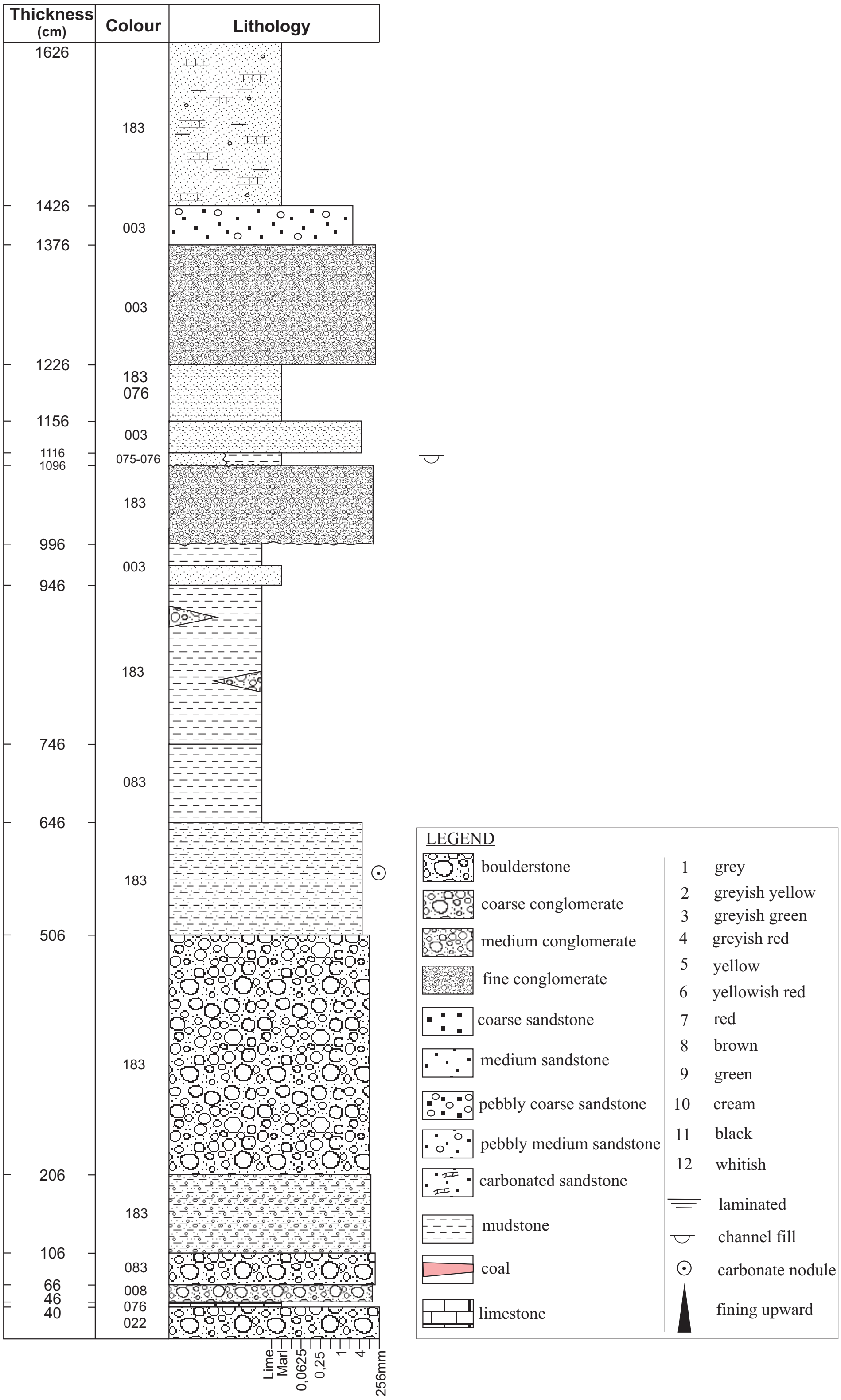

Figure 4. Partial type sections of the Ayaklıkırı Formation, location II (see Figure 3 for location).

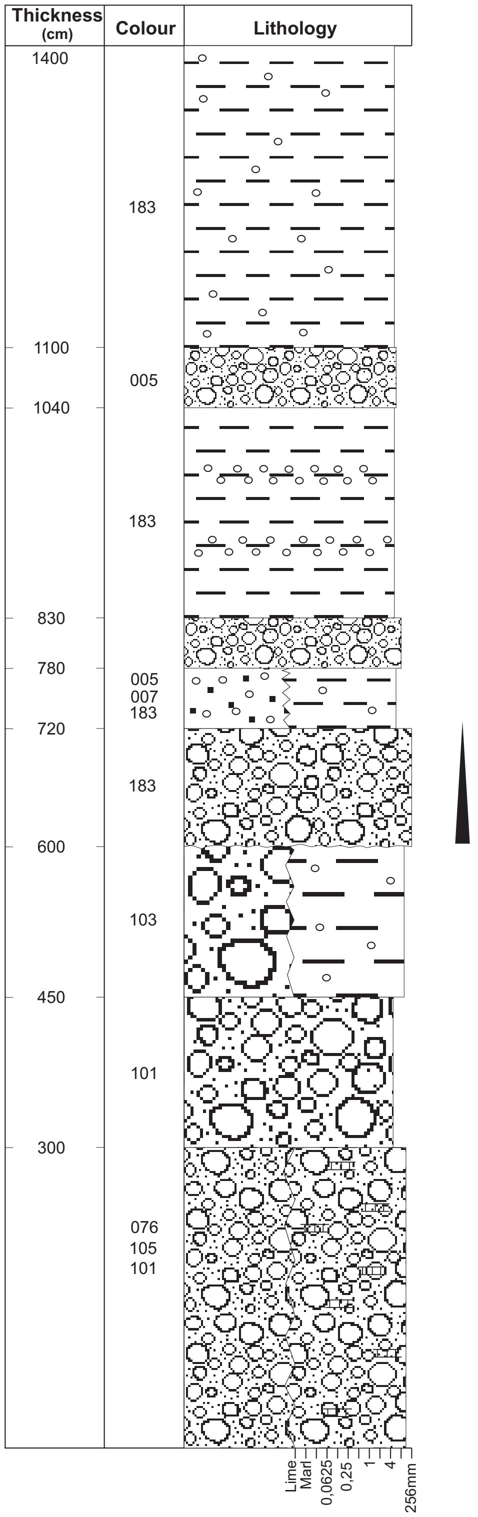

Figure 5. Partial type sections of the Ayaklıkırı Formation, location I (see Figure 3 for location and Figure 4 for legend).

small vein (Figure 6), 565 cm in medium vein (Figure 7) and 1020 cm in large vein (Figure 8).

At the base of the Ayaklıkırı Formation are limestones and clayey, sandy, gravelly limestones which include fresh-brackish water algae fossils, and in some areas are associated with conglomerates. Red-pink, cream-beige lacustrine (algal) limestones that precipitated on the basement display various thicknesses. They grade into marls and some fine gravelly limestones and conglomerates. The components of the gravelly limestones are derived from basement units and covered by algal bioherms. These clasts are angular and sub-rounded. The gravels are on average pebble (a few mm to 3–4 cm) sized, with 10% boulder sized. In some places, basal limestones pass upward into conglomerates which are cemented by pure carbonates and some clayey or sandy carbonate. The angular gravels in these horizons are generally 2–4 cm in size and occasionally reach a maximum size of 25 cm. These conglomerate levels have some dusty white sandstone or greenish grey mudstone interlayers.

Grey-yellow-beige or light red, milky brown, lithified, poorly to moderately sorted basal conglomerates have clay-sand matrix and are cemented by algal limestones. The sizes of the components range between coarse sand and boulder (50–60 cm). Most of the gravels were crusted by carbonate. Conglomerates locally include claystone-mudstone, gravelly algal limestone, gravelly mudstone or algal limestone beds less than 3–5 cm thick.

Carbonate Sedimentology– The carbonate levels of the Ayaklıkırı Formation are represented by terrestrial and shallow fresh or brackish water lacustrine carbonates interbedded with pebbly calcarenitic sandstones. The terrestrial and lacustrine carbonates can be divided into 6 different types: (1) silty clayey laminated micritic carbonates, (2) silty and clayey fenestral pore-bearing laminated microbial carbonates, (3) bioturbated algal carbonate crusts, (4) peloidal microbial carbonates, (5) ostracod-bearing microbial micritic carbonates and (6) pebbly-sandy clayey micritic carbonates (Plates I–IV).

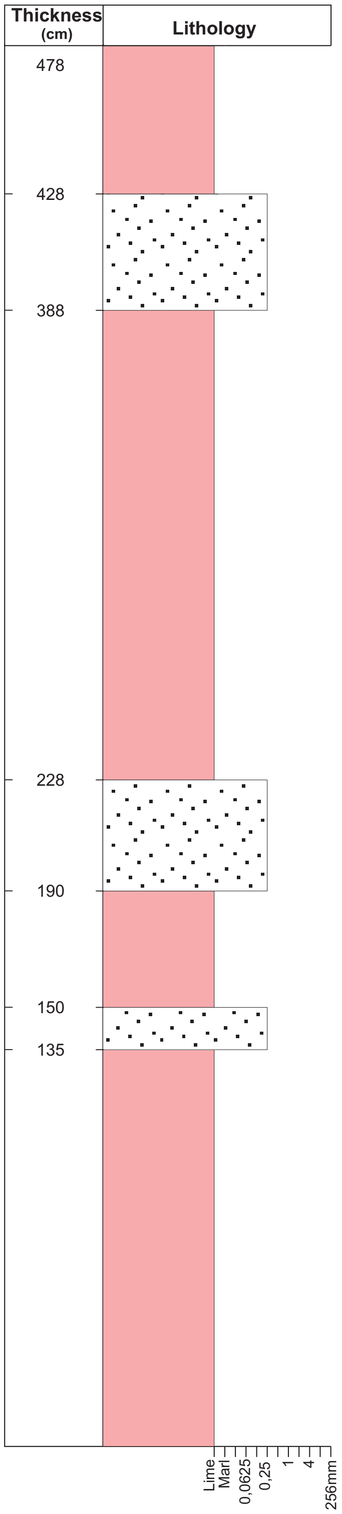

Figure 6. Coal bearing partial type sections of the Ayaklıkırı Formation, small seam, location III (see Figure 3 for location and Figure 4 for legend).

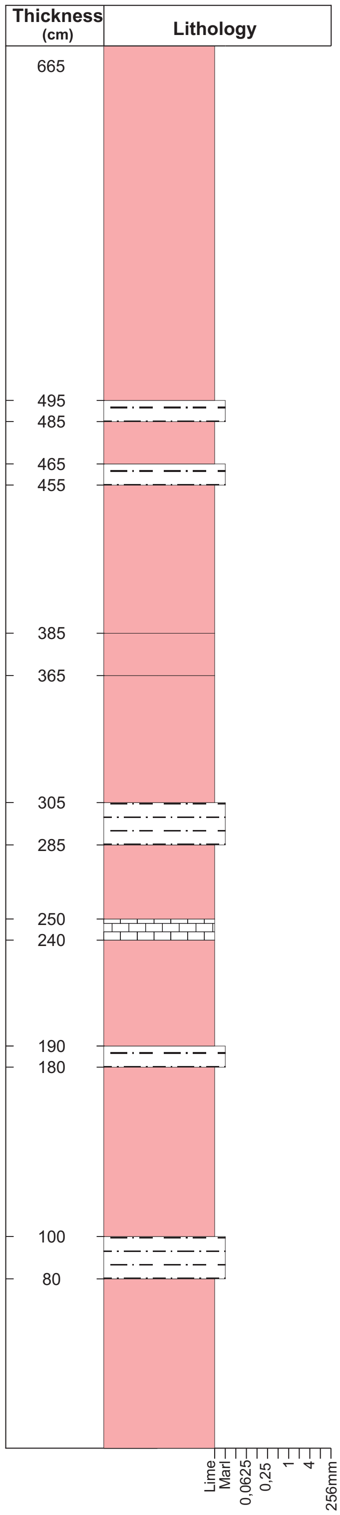

Figure 7. Coal-bearing partial type sections of the Ayaklıkırı Formation, medium seam, location III (see Figure 3 for location and Figure 4 for legend).

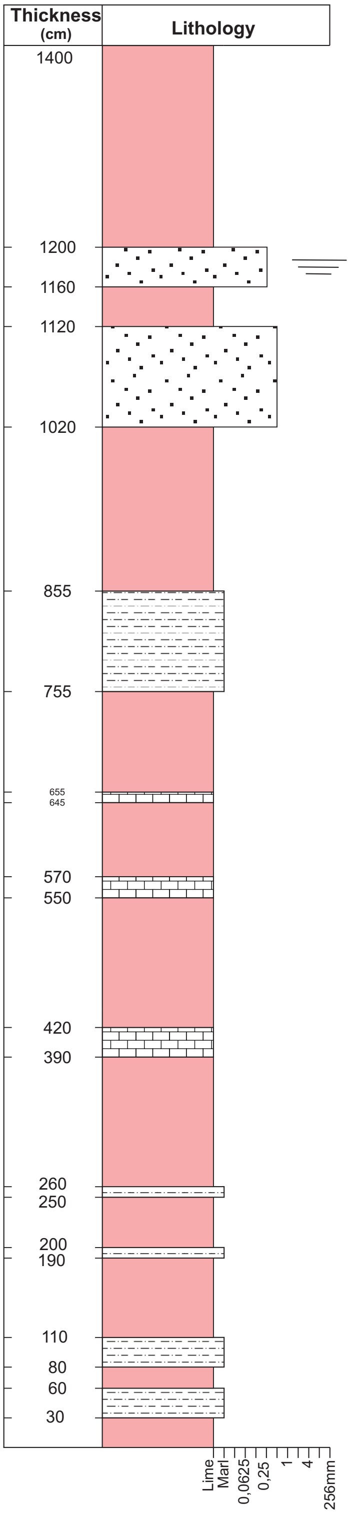

Figure 8. Coal-bearing partial type sections of the Ayaklıkırı Formation, large seam, location III (see Figure 3 for location and Figure 4 for legend).

The pebbly calcarenitic sandstones consist of red, yellowish red, pinkish yellow, laminated or non-laminated thin pebble-bearing calcarenitic sandstones. The sandstones are composed entirely of marble sands which are derived from the marble of the basement. The sands are moderately or well sorted, subprismoidal to spherical in shape and angular to subangular. The matrix is commonly composed of pseudospar calcite cement, or rarely iron oxidized clay. The moderate- or well-sorted sandstone grains are relic of the coarse granoblastic texture of the marble source rock (Plate 2, Figures 1 & 4).

The terrestrial and shallow fresh water lacustrine carbonates are characterized by six different carbonate types.

(1) Silty clayey laminated micritic carbonates (carbonate mudstone) are made up of pinkish red, yellowish light brown, slightly undulating, very thin laminated, iron oxide-bearing, sandy and silty, clayey micritic limestone. The carbonate sequence includes iron oxide-bearing small erosion surfaces which are parallel to lamination and include bioturbation traces (Plate 1, Figure 6). Silt grains are composed of quartz, feldspar and very thin mica flakes lying parallel to lamination planes (Plate 1, Figures 1, 2, 3 & 6; sample no ET-1 and ET-2).

(2) Silty and clayey, fenestral pore-bearing laminated microbial carbonates (microbial carbonate mudstone), consist of red, yellowish light brown, slightly undulating very thin laminated, sand and silt-bearing clayey algal micritic limestone. The facies is characterized by abundant laminated fenestral carbonates with pores filled with sparry calcite. Sand and silt grains are commonly composed of single crystal or polycrystalline quartz with rare feldspar grains. The facies frequently lies on the silty clayey laminated micritic carbonates along an erosional surface (Plate 1, Figures 5 & 6; Plate 2). Wavy lamination and dark micritic carbonates reflects an algal-microbial origin.

(3) Bioturbated algal carbonate crust (bindstone), characterized by yellow to light brown, laminated or non-laminated, extremely bioturbated, rhisolith-bearing algal micritic

carbonate and red, or orange micritic and microsparitic carbonate crust. Algal micrite can be recognized by its dark colouring in thin sections (Plate 2, Figures 6, 7 & 8; Plate 4, Figures 1 & 2).

(4) Peloidal microbial carbonate (bindstone) is composed of yellowish light brown to brown, layered algal peloidal micrite frame and spar calcite pore fill (Plate 4, Figures 3, 4 & 5).

(5) Ostracod bearing microbial micritic carbonates (microbial carbonate mudstone) consist of brown, layered, irregularly dispersed small irregular fenestrae and ostracod-bearing microbial micrite (Plate 4, Figure 8).

(6) Pebbly-sandy, clayey micritic carbonates (carbonate mudstone) are recognized as yellowish pink, indistinctly layered lithologies, composed of micritic carbonate containing pebble to sand sized metamorphic rock fragments (Plate 3, Figures 5 & 6; Plate 4, Figures 6 & 7). Pebbles and sands are composed of marble and schist fragments sourced from the Menderes Massif and Cycladic Complex.

The pebbly calcarenitic sandstones are commonly present in the lower beds of the carbonate sequence directly above the basement rocks. However at one location terrestrial and lacustrine carbonates may directly overlie the basement rocks (Plate 3, Figure 1).

Interpretation of Lithofacies, Carbonate Environment– The iron-oxidized clay matrix and the red or orange colour of the pebbly calcarenitic sandstones reflects terrestrial oxidizing conditions for the basal pebbly calcarenitic sandstones. The angular to subangular shape of sands, poor grain orientation and organization reflects restricted transport.

Iron oxide-bearing small erosion surfaces, bioturbation traces (Plate 1, Figure 6) and the sand, silt and clay content of the silty clayey laminated micritic carbonate (carbonate mudstone) facies indicates a playa like very shallow lacustrine environment affected by subaerial conditions.

The laminated fenestral pore structures of silty and clayey, fenestral pore-bearing laminated microbial carbonates (microbial carbonate mudstone) show evidence of shrinkage cracks (Plate 2; Plate 3, Figure 5) indicating very shallow water and repetitive subaereal conditions (Plate 1, Figures 4–7).

Rhisolith-bearing and extremely bioturbated algal micrites of the bioturbated algal carbonate crust (bindstone) (Plate 2, Figures 6–8; Plate 4, Figures 1 & 2), facies might have been precipitated in very shallow basins in wetland areas.

The microbial micritic frame of the Peloidal microbial carbonate (bindstone) (Plate 4, Figures 3–5) facies may indicate relatively deeper water (a metre to a few metres) conditions and rapid carbonate precipitation, forming the peloidal carbonate-frame formation.

Ostracod-bearing microbial micritic carbonate (microbial carbonate mudstone) (Plate 4, Figures 8) facies may indicate relatively deeper lacustrine (a metre to a few metres) conditions.

Poorly oriented, sparsely scattered, poorly sorted and angular pebble and sand contents and shrinkage cracks of pebbly-sandy, clayey micritic carbonates (carbonate mudstone) facies (Plate 3, Figures 5 & 6; Plate 4, Figures 6 & 7) suggests restricted terrestrial supply and sedimentation in shallow and very stagnant water.

As seen in Plate 1 (Figure 6) and Plate 3 (Figures 2–4), silty clayey laminated micritic carbonates, silty or clayey fenestral pore-bearing laminated microbial carbonates and bioturbated algal carbonate crust facies constitute an alternating carbonate sequence indicating slight changes (a metre to a few metres) in water depth in a lacustrine environment. The peloidal microbial carbonates and ostracod-bearing microbial micritic carbonate facies appear in the middle and upper parts of the carbonate sequence. Hence this very shallow Neogene carbonate basin shows sporadic deepening over time.

All observations and evidence mentioned above indicates that carbonates of the Ayaklıkırı Formation have precipitated in a fresh or brackish water playa or wetland area, such as a very shallow lacustrine environment affected by subaereal conditions, to a relatively deeper, very stagnant shallow lake. Rare gravel to boulder sized angular clasts in the stagnant water limestones indicate short transport by a low energy stream.

Interpretation of Lithofacies, Detritus Environment– Sediment transport into the basin started shortly after the deepening. Poorly lithified coarse sand, pebble and boulder layers occurred with lateral and horizontal transitions. The texture and the geometry of the conglomerates indicate an alluvial fan environment which developed on the slopes, controlled by the high energy streams, allowing rapid material accumulation. Carbonate cement in some grain supported conglomerates indicates that the carbonate precipitation was still continuing during the detrital influx.

Excessive transport led the fluvial sediments to become dominant during the later stages of the Ayaklıkırı Formation. Fluvial deposition is mainly represented by channel fills and flood plain sediments. Marl interbeds within the superposed channel fills indicate seasonal floods.

The coal beds around the Akçaşehir area occurred where the basin had local swampy conditions (see Palynological Data below for the detailed interpretation of the coal beds and their environment)

Aydoğdu Formation

This formation was observed mainly around Tire and Karatekkeköy and covers a total area of 13 km^2 (Figure 3). It is generally dusty white-light grey, reddish brown, poorly lithified and principally composed of conglomerates and sandstones.

Conglomerates are more abundant than sandstones. In some areas conglomerates and sandstones display transition to gravelly sandstones or are interbedded with them. Because of the close lithological resemblance of the foregoing rocks and the Aydoğdu Formation (Emre *et al.* 2006a, b) we have used the same lithostratigraphic unit name. Because farmland obscured the incompetent formation with moderately mature texture, there was no chance of analysing a stratigraphic section.

Description of Lithofacies– Conglomerates are poorly to moderately lithified and medium-thick bedded. The clasts display an immature to moderately mature texture and are very poorly sorted. Sediments have angular, some sub-angular or platy shapes with low sphericity. Most (up to 95%) of the clasts are composed of metamorphic rocks and meta-olistostromes; this varies according to the area of deposition. The sizes of the gravel clasts range from granules to boulder: most are dominantly pebbles and cobbles but rare boulders are present. Matrix-supported conglomerates with generally irregular internal structure have clay to granule sized matrix. Coarsening upward is common. The unit occasionally includes coarse grained, thin sandstone lenses.

Sandstones are light brown, moderately lithified, generally coarse grained and medium to thick bedded. Locally, scattered gravel-bearing sandstones fine upwards. The percentage of scattered gravel within the gravelly sandstones is less than 5%.

The poorly sorted basal conglomerates of the Aydoğdu Formation possess no obvious bedding, have a coarse sand-granule matrix and unconformably overlie the basement and the Ayaklıkırı Formation. These conglomerates contain generally angular clasts varying in size from granule to boulder.

The palynological samples taken from rare, fine-grained beds in the succession are barren. Lacking palaeontological evidence, the age of the Aydoğdu Formation was assumed to be Plio–Pleistocene (?) by Emre *et al.* (2006a, b).

Interpretation of Lithofacies– Concomitance of the sand and boulder sized clasts within conglomerates and deposition of the sand and fine gravels in front of the boulders with regard to the palaeocurrent indicate that the formation developed in an alluvial fan environment on the slopes.

Scattered pebbles in the sandstones, variation of bed thicknesses and the limited number of the palaeocurrent-induced sedimentary structures indicate that streams with high energy flows controlled the alluvial fan deposition and allowed rapid sediment accumulation. However, some current-related structures such as cross-bedding record calmer periods of stream-flow.

Deposition of the Aydoğdu Formation was controlled by high-angle normal faults concurrent to the high energy streams.

Alluvium

Grey-beige alluvium is composed of various sediments including various sizes of gravel with clay-silt-sand matrix. The unit constitutes vast plains which are found in topographically lower parts of the study area. These unlithified sediments, deposited by recent streams and composed of disordered, various sized clastics, overlay all units unconformably.

Palynological Data

Eight palynological samples were obtained from the Ayaklıkırı Formation in the Tire area. The palynoflora of the investigated samples from the Tire area show poor preservation of spores and pollen. It was therefore impossible to count the palynomorphs per slide. Here we have just prepared a list showing the palynomorph assemblage of Tire lignites. Palynological data provide information on the age of deposition as well as palaeoclimate and palaeoenvironmental conditions.

In this study, 22 genera and 21 species have been described (Table 1, Plate V). The low numbers of palynomorphs should be related to ph conditions, bad preservation or depositional environment. The species recorded in Table 1 commonly occur in the Neogene sediments of Turkey (e.g., Akgün & Akyol 1999; Akgün *et al.* 2007; Kayseri & Akgün 2008). Additionally, the content of species obtained is similar to the content of palynomorphs obtained from other Turkish Middle Miocene sediments (e.g., Akgün *et al.* 1986; Akyol & Akgün 1990; Akgün & Akyol 1999; Kayseri & Akgün 2008). The spore species show little diversity (Table 1). Moreover, the plicoid species *Plicatopollis plicatus* that generally occurs in Eocene and Oligocene sediments is also present in the assemblage. Some subtriporate pollens (e.g., *Subtriporopollenites constans* and *Subtriporopollenites anulatus* ssp. *Nanus)* have been inherited from the 'early' Tertiary and have also been recorded from the Tire lignites. However, some *Periporopollenites* sp. (Chenopodiaceae) also occurs in the samples, but is rarer. In general, the abundance of Gramineae, Compositae, Chenopodiceae and Cyperaceae was relatively lower during the Early–Middle Miocene in Turkey (Akgün *et al.* 2000, 2007). However, high percentages of these species were recorded from the Oligocene–Miocene sediments in Eastern Turkey (Sancay *et al.* 2006; Batı & Sancay 2007). From the Late Miocene onward, they increase in abundance and percentages continually rise up to the top (Akgün *et al.* 2000). The lignite-bearing parts of the sediments in the Tire area were deposited during the latest Early Miocene–earliest Late Miocene period on the basis of both palynological data and mammal data (Becker-Platen *et al.* 1975; Kaya 1987).

In terms of palaeoenvironment, qualitative analyses of the palynoflora indicate that swamps including Taxodiaceae, Myricaceae and ferns occur adjacent to lake surrounded by topographic highs covered by forests such as Fagaceae, *Quercus* and *Pinus*. In the lake, *Planorbis* sp. and *Limnea* sp. lived (Özcan 1984). Lowland-riparian elements are characterized by the presence of Juglandaceae, *Carya*, *Alnus*, *Ulmus*, Cyrillaceae, *Castanea* and Sapotaceae. Open vegetation species Chenopodiaceae occur in the open grassland.

Palaeoclimate

Quantitative terrestrial palaeoclimatic analysis on the basis of the palynological assemblage of the Tire lignites was carried out using the Coexistence Approach proposed by Mosbrugger & Utescher (1997): this technique relies on the nearest living relative philosophy, based on the assumption that climatic requirements of Tertiary plant taxa are similar to those of their living relatives (Mosbrugger & Utescher 1997).

An initial survey of the sample material showed that the palynoflora of samples taken from the Tire lignites were not remarkably different from each other. However, as indicated in the palynological data, we have a limited palynological assemblage. Our palynoflora have been analysed with respect to seven climate parameters (for explanation of abbreviations see Table 2).

Table 1. Species list of pollen and spores from the Tire lignites.

FOSSIL TAXA	BOTANICAL AFFINITY
Spores	
Polypodiaceoisporites marxheimensis (Mürriger & Pflug ex Thomson & Pflug) Krutzsch	Schizaeaceae? Dicksoniaceae?, Pteridaceae?
Polypodiaceoisporites sp.	
Retitriletes sp.	
Punctatisporites sp.	
Laevigatosporites haardti (Potonié & Venkatachala) Thomson & Pflug	Polypodiaceae
Pollen	
Sequoiapollenites polyformosus Thiergart	*Sequoia*
Cyacadopites sp.	Cyacadaceae
Ephedripites sp.	Ephedraceae
Inaperturopollenites dubius (Potonié & Venkatachala) Thomson & Pflug	Taxodiaceae
Cupressacites insulipopillatus (Trevisan) Krutzsch	Cupressaceae
Pityosporites microalatus (Potonié) Thomson & Pflug	Pinaceae; *Pinus* haploxyon tip
Pityosporites spp.	
Podocarpidites libellus (Potonié) Krutzsch	Podocarpaceae; *Podocarpus*
Triporopollenites labraferus (Potonié) Thomson & Pflug	
Triatripollenites rurensis Pflug & Thomson *in* Thomson & Pflug	Myricaceae; *Myrica*
Momipites punctatus (Potonié) Nagy	*Engelhardia*
Subtriporopollenites constans Pflug *in* Thomson & Pflug	
Subtriporopollenites anulatus Thomson & Pflug ssp. *nanus* Thomson & Pflug	Juglandaceae; *Carya*?
Caryapollenites simplex (Potonié) Thomson & Pflug	*Carya cordiformis*
Plicatopollis plicatus (Potonié) Krutzsch	Juglandaceae
Polyvestibulopollenites verus (Potonié) Thomson & Pflug	Betulaceae; *Alnus*
Polyporopollenites undulosus (Woff) Thomson & Pflug	Ulmaceae; *Ulmus*?, Zelkova?
Tricolpopollenites microhenrici (Potonié) Thomson & Pflug	Fagaceae; ? *Quercus*
Tricolpopollenites retiformis Pflug & Thomson *in* Thomson & Pflug	*Salix/Platanus*
Tricolpopollenites henrici (Potonié) Thomson & Pflug	Fagaceae; ?*Quercus*
Tricolpopollenites densus Pflug *in* Thomson & Pflug	*Quercus*
Tricolporopollenites megaexactus Potonié	Cyrillaceae
Tricolporopollenites microreticulatus Pflug & Thomson *in* Thomson & Pflug	Oleaceae
Tricolporopollenites cingulum (Potonié) Thomson & Pflug ssp. *pusillus* (Potonié) Thomson & Pflug	Castanae, *Castanopsis*
Periporopollenites multiporatus Pflug & Thomson *in* Thomson & Pflug	Chenopodiaceae
Periporopollenites sp. (thallictrum type)	Chenopodiaceae
Tetracolporopollenites sp.	Sapotaceae

Table 2. List of climate parameters and abbreviations used in this paper.

Mean annual temperature (^{0}C)	MAT
Temperature of the coldest month (^{0}C)	CMT
Temperature of the warmest month (^{0}C)	WMT
Mean annual precipitation (mm)	MAP
Precipitation of the wettest month	HMP
Precipitation of the driest month	LMP
Precipitation of the warmest month	WMP

Table 4. Species list of the megaflora from the Tire lignites (Gemici *et al.* 1992).

Acer trilobatum (Stbg.) A.Br.	*Phragmites* sp.
Buxus sempervirens L.	*Populus latior* A.Br.
cf. *Cassia* sp.	cf. *Quercus goepperti* Weber
Cinnamomum polymorphum Heer	cf. *Quercus* cf. *neriifolia* A.Br.
Cornus sp.	*Quercus* sp.
Fraxinus sp.	*Sapindus falcifolius* A.Br.
Pinus sp.	*Salix* sp.
	Typa sp.

Because the palynological assemblage has a low species diversification, the climatic evaluation is based on 14 taxa (Table 3). Quantitative results show that the values for the MAT are between 16.5–21.3 °C, 5.5–13.3 °C for the CMT, 27.3–28.1 °C for the WMT and 887–1520 mm for the MAP. Calculations of the HMP yield an interval from 204 to 225 mm. The values obtained are between 16 and 43 mm for the LMP and 51 and 61 mm for the WMP.

In addition, we also evaluated the Middle Miocene megaflora from the same formation determined by Gemici *et al.* (1992). The megaflora consists of 15 taxa (Table 4). Here, the palaeoclimatic reconstruction is based on 7 taxa. The resulting coexistence interval for the MAT ranges from 14.4 to 17.3 °C. The second coexistence interval appears at 20.6–20.8 °C (Table 5). These two coexistence intervals probably define two different plant communities that grew under discrete climatic conditions formed by variations in local geography. The interval for the TCM is rather broad and ranges from 3.7 to 10.8 °C. Calculations of the TWM yield an interval from 26.4 to 26.7 °C. For the MAP, the coexistence approach yields values between 867 and 1333 mm. The range of precipitation in the wettest month is determined to be between 116 and 141 mm. The interval for the LMP is reasonable wide ranges from 32 to 70mm, and the WMP is suggested to lie between 81 and 86 mm (Table 5).

In general, the Coexistence Approach on the basis of palynoflora yields a wider coexistence interval than on leaf flora (Mosbrugger & Utescher 1997; Liang *et al.* 2003). This is believed to be related to the fact that nearest living relatives of Tertiary palynomorphs are frequently determined only to family whereas nearest living relatives of Tertiary leaves are more reliably identified to specific and generic level (Mosbrugger & Utescher 1997). The lower floral diversity provides a wide coexistence interval leading to a lower climatic resolution. However, temperature values based on leaf data from the Tire lignites are obtained from 7 taxa and hence there is a lower climatic resolution.

The climate data obtained are correlated with previous studies made in coeval sediments in Turkey. Using palynological data, the first comprehensive palaeoclimate reconstruction on Neogene deposits was made by Akgün *et al.* (2007). The authors

Table 3. Coexistence intervals of palynoflora obtained from the Tire lignites.

Climate parameter	Climate value	Bordering taxa
MAT	16.5–21.3 °C	Cycadaceae–*Carya cordiformis*
TCM	5–13.3 °C	Cycadaceae–*Carya cordiformis*
TWM	27.3–28. 1 °C	Cycadaceae–Taxodiaceae
MAP	887–1520mm	Cycadaceae–Taxodiaceae
HMP	204–245mm	*Engelhardia*–Taxodiaceae
LMP	16–43mm	Podocarpaceae–Cupressaceae
WMP	51–61mm	Sapotacaeae–*Ephedra*

obtained the latest Burdigalian (late Early Miocene) palaeoclimate data from the Emet, Kırka and Kestelek localities of the Bigadiç Basin (Western Anatolia) and indicated a MAT between 17 and 21.3 °C, a TCM between 6.2 and 13.3 °C, a TWM between 26.5 and 27.9 °C and a MAP between 1217 and 1322 mm (Table 6).

For central Anatolia, the data obtained from the Samsun Havza area indicate that the palaeotemperature values are between 17.2 and 20.8 °C for the MAT, 6.2 and 13.3 °C for the TCM, 27.3 and 27.9 °C for the TWM, and rainfall was 1217 and 1322 mm for the MAP (Akgün *et al.* 2007). Akgün *et al.* (2007) also calculated the palaeoclimatic values for the Langhian (Middle Miocene) from the Aydın area (Başçayır and Kuloğulları). The data obtained are between 17 and 21.3 °C for the MAT, 6.2 and 13.3 °C for the TCM, 26.5 and 28.1 °C for TWM, and 1183 and 1322 mm for the MAP (Table 6). When we compare palaeoclimate data from Akgün *et al.* (2007) with the data obtained from the palyno and leaf flora of Tire lignites, the coexistence intervals in the MAT, TCM and TWM mostly overlap. However, it is necessary to indicate that the lower boundaries of the MAT and TCM in the Tire lignites are lower than in the palaeoclimate data of Akgün *et al.* (2007). Also, the lower boundary of the MAP for the Tire lignites is below 1000 mm (Table 6). Typically the resolution and the reliability of the resulting coexistence intervals increase with the number of taxa included in the analysis and are relatively high in floras with 10 or more taxa for which climate parameters are known. Since the flora obtained have low species diversification, related climatic parameters are characterized by wide coexistence interval.

Table 5. Coexistence intervals of the Tire lignites leaf flora.

Climate Parameter	Climate Value	Bordering Taxa
MAT	14.4–17.3 °C	*Quercus incana–Buxus sempervirens*
	20.6–20.8 °C	*Cassia–Acer sacharinum*
TCM	3.7–10.8 °C	*Quercus incana–Buxus sempervirens*
TWM	26.5–26.7 °C	*Cassia–Buxus sempervirens*
MAP	867–1333 mm	*Sapindus–Buxus sempervirens*
HMP	116–141 mm	*Sapindus–Buxus sempervirens*
LMP	32–70 mm	*Sapindus–Acer sacharinum*
WMP	81–86 mm	*Sapindus–Buxus sempervirens*

Table 6. Coexistence intervals of the calculated climatic parameters and correlation with previous study of Akgün *et al.* (2007).

MAT(°C)	TCM (°C)	TWM (°C)	MAP (mm)	
Tire palynoflora	16.5–21.5	5–13.3	27.3–28.1	887–1520
Tire megaflora (Gemici *et al*. 1992)	14.4–17.3 20.6–20.8	3.7–10.8	26.5–26.7	867–1333
Bigadiç Basin (Akgün *et al*. 2007)	17–21.3	6.2–13.3	26.5–27.9	1217–1322
Samsun–Havza Area (Akgün *et al*. 2007)	17.2–20.8	6.2–13.3	27.3–27.9	1217–1322
Aydın(Başçayır–Kuloğulları) (Akgün *et al*. 2007)	17–21.3	6.2–13.3	26.5–28.1	1187–1322

Palaeoclimatic values thus indicate a warm temperate and humid climate with a small variation in precipitation; these climate values represent the climatic conditions preceding the Middle Miocene Climatic Optimum (MMCO) defined by isotopic data (Zachos *et al.* 2001, 2008). According to Mosbrugger *et al.* (2005), temperatures rose in the later Burdigalian. The following warm period continued until the earlier part of the Serravallian, and corresponds with the global MMCO.

Discussion and Conclusion

The Ayaklıkırı Formation, Aydoğdu Formation and alluvium unconformably overlie the basement rocks. The Ayaklıkırı Formation contains both lateral and vertical transitions with bedded lacustrine and fluvial sediments. The base of the formation is composed of terrestrial to shallow, stagnant, fresh or brackish water lake carbonates including ostracod and algal limestones found on the metamorphic basement. The carbonates are laterally discontinuous and are laterally and vertically intercalated with alluvial fan deposits controlled by fluvial systems.

The stratigraphic succession around Tire shows important differences from the successions in the Kiraz-Beydağ (Emre *et al.* 2006b) Ödemiş (Emre 2007) and Bayındır (Emre *et al.* 2006a) areas. Palaeontological and lithological evidence suggests independent deposition in the sub-basins within the Küçük Menderes Graben, as mentioned in Rojay *et al.* (2001, 2005).

An angular unconformity between the Ayaklıkırı and Aydoğdu formations indicates lack of sedimentation during the latest Late Miocene. A new stage of fluvial sedimentation controlled by the high angle normal faults started after this pause.

Alluvium deposited in topographic lows after the Pleistocene rests unconformably on the other units.

The palynological assemblage obtained from the coals of the Ayaklıkırı Formation generally consists of taxa that commonly occur in the Middle Miocene sediments of Turkey. However, the species *Plicatopollis plicatus*, *Subtriporopollenites constans* and *S. anulatus nanus* are inherited from the older Tertiary sediments. The pollen of Gramineae, Compositae, Chenopodiaceae and Cyperaceae, which show an increase in abundance at the beginning of the Late Miocene, are otherwise rarely present in the assemblage. Palynological data indicate that the coal beds of the Ayaklıkırı Formation were deposited during the latest Early Miocene–earliest Late Miocene period.

Palaeoclimatic results obtained indicate a warm temperate and humid climate, and values obtained indicate a warm temperate climate preceding the global Middle Miocene Climatic Optimum.

Acknowledgements

This study was supported by Dokuz Eylül University, AFS Project, No. 04. KB. FEN.032 awarded to Tahir Emre. The authors would like to express their gratitude to Robert Thorne who read the whole manuscript and forwarded his remarks. Special thanks go to Funda Akgün for her valuable contributions during the identification of palynomorphs. We would also like to thank Reşit Altınöz who drew some figures and to the Tire Lignite Company for permitting us to sample from their coal deposit. This paper has also benefited from comments and suggestions by the referees and the editor.

References

Akgün, F., Alişan, C. & Akyol, E. 1986. Soma Neojen stratigrafisine palinolojik bir yaklaşım [A palynological approach to the Neogene stratigraphy of Soma]. *Türkiye Jeoloji Kurumu Bülteni* **29**, 13–25 [in Turkish with English abstract].

Akgün, F. & Akyol, E. 1999. Palynostratigraphy of the coal-bearing Neogene deposits graben in Büyük Menderes Western Anatolia. *Geobios* **32**, 367–383.

Akgün, F., Kaya, T., Forsten, A. & Atalay, Z. 2000. Biostratigraphic data (mammalia and palynology) from the Upper Miocene İncesu formation at Düzyayla (Hafik, Sivas, central Anatolia). *Turkish Journal of Earth Sciences* **9**, 57–67.

Akgün, F., Kayseri, M.S. & Akkiraz, M.S. 2007. Paleoclimatic evolution and vegetational changes during the Late Oligocene–Miocene period in western and central Anatolia (Turkey). *Palaeogeography, Palaeoclimatology, Palaeoecology* **253**, 56–106.

AKYOL, E. & AKGÜN, F. 1990. Bigadiç, Kestelek, Emet ve Kırka boratlı Neojen tortullarının palinolojisi ve karşılaştırılması [Palynology and correlation of borate-bearing Neogene deposits from Bigadiç, Kestelek, Emet and Kirka]. *Mineral Research and Exploration Institute of Turkey (MTA) Bulletin* **111**, 165–175 [in Turkish with English Abstract].

ANGELIER, J., DUMONT, J.F., KARAMANDERESİ, İ.H., POISSON, A, ŞİMŞEK, Ş., & UYSAL, Ş. 1981. Analyses of fault mechanisms and expansion of southwestern Anatolia since the Late Miocene. *Tectonophysics* **79**, 11–19.

BATI, Z. & SANCAY, H. 2007. Palynostratigraphy of Rupelian sediments in the Muş Basin, Eastern Anatolia, Turkey. *Micropaleontology* **53**, 249–283.

BECKER-PLANTEN, J.D., SICKENBERG, O. & TOBIEN, H. 1975. Vertabraten Lokalfaunen Der Turkei un ihre Altersstellung. *In:* SICKENBERG, O. (ed), *Die Gliederung Des Höheren Jungtertiárs und Altquartáre in der Turkei nach Vertebraten un Ihre Bedeutung für die Internationale Neogen-Stratigraphie*. Geologisches Jahrbuch **B15**, 47–100.

BOZKURT, E. & ROJAY, B. 2005. Episodic, two-stage Neogene extension and short-term intervening compression in western Anatolia: field evidence from the Kiraz Basin and Bozdağ Horst. *Geodinamica Acta* **18**, 295–312.

CANDAN, O., DORA, O.Ö., OBERHÄNSLI, R., ÇETİNKAPLAN, M., PARTZSCH, J. H., WARKUS, F. C. & DÜRR, S. 2001. Pan-African high-pressure metamorphism in the Precambrian basement of the Menderes Massif, western Anatolia, Turkey. *International Journal of Earth Sciences* **89**, 793–811.

CANDAN, O., DORA, O.Ö., OBERHÄNSLI, R., OELSNER, F. & DÜRR, S. 1997. Blueschist relics in the Mesozoic cover series of the Menderes Massif and correlations with Samos Island, Cyclades. *Schweizerische Mineralogische und Petrographische Mitteilungen* **77**, 95–99.

CANDAN, O., OBERHÄNSLI, R., ÇETİNKAPLAN, M. & RIMMELÉ, G. 2007, Batı Anadolu'da yüzeyleyen Menderes Masifi ve Kikladik Kompleks'e ait birimlerin litostratigrafi, metamorfizma ve tektonik evrim açısından tanımlanması [Description of the Menderes Massif and Cycladic Complex in Western Anatolia in terms of their lithostratigraphic, metamorphic and tectonic evolution]. *Abstracts, 61. Türkiye Jeoloji Kurultayı, Ankara*, p. 233 [in Turkish and English].

ÇETİNKAPLAN, M. 2002. *Tertiary High Pressure/Low Temperature Metamorphism in the Mesozoic Cover Series of the Menderes Massif and Correlation with the Cycladic Crystalline Complex.* PhD Thesis, Dokuz Eylül University, İzmir, Turkey [unpublished].

DEWEY, J.F. & ŞENGÖR, A.M.C. 1979. Aegean and surrounding regions: complex multiple and continuum tectonics in a convergent zone. *Geological Society of America Bulletin* **90**, 84–92.

DUMONT, J.F., UYSAL, Ş., ŞİMŞEK, Ş., KARAMANDERESİ, İ.H. & LETOUZEY, J. 1979. Güneybatı Anadolu'daki grabenlerin oluşumu [Formation of the grabens in Southwestern Anatolia]. *Mineral Research and Exploration Institute of Turkey (MTA) Bulletin* **92**, 7–17 [in Turkish].

EMRE, T. 2007. Neogene–Quaternary stratigraphy and tectonics of Ödemiş-Kaymakçı surroundings, Küçük Menderes Graben, western Anatolia. *Çukurova Univesity, Geological Engineering Department, 30th Anniversary Symposium, Abstracts*, 183–184.

EMRE, T. & SÖZBİLİR, H. 2005. Geology, Geochemistry and Geochronology of the Başova Andesite, Eastern end of the Küçük Menderes Graben. *Mineral Research and Exploration of Turkey (MTA) Bulletin* **131,** 1–19 [English edition].

EMRE, T. & SÖZBİLİR, H. 2007. Tectonic Evolution of the Kiraz Basin, Küçük Menderes Graben: Evidence for compression/uplift-related basin formation overprinted by extensional tectonics in West Anatolia. *Turkish Journal of Earth Sciences* **16**, 441–470.

EMRE, T., RÜZGAR, Y. & SÖZBİLİR, H. 2006a. Neogene–Quaternary stratigraphy and tectonics of the Küçük Menderes Graben, around Bayındır-Kiraz, West Anatolia. *30. Anniversary of Fikret Kurtman Geology Symposium, Abstracts*. Selçuk University, Konya, 5–6.

EMRE, T., SÖZBİLİR, H. & GÖKÇEN, N. 2006b. Neogene–Quternary stratigraphy of Kiraz-Beydağ region, Küçük Menderes Graben, West Anatolia. *Mineral Research and Exploration of Turkey (MTA) Bulletin* **132,** 1–32 [English edition].

EMRE, T., SÖZBİLİR, H., GÖKÇEN, N. & AKGÜN, F. 2003. Kiraz (İzmir) kuzeydoğusunun jeolojisi, Küçük Menderes Grabeni, Batı Anadolu [Geology of NE of Kiraz (İzmir), Küçük Menderes Graben, Western Anatolia]. *56. Türkiye Jeoloji Kurultayı Bildiri Özleri Kitabı,* Ankara, 87–88.

ERCAN, T., SATIR, M., SERİN, D. & TÜRKECAN, A. 1996. Batı Anadoludaki Tersiyer ve Kuvaterner yaşlı volkanik kayaçlarda yeni yapılan radyometrik yaş ölçümlerinin yorumu [Interpretation of the new geochemical, isotopic and radiometric data from the western Anatolian Tertiary and Quaternary volcanic rocks]. *Mineral Research and Exploration of Turkey (MTA) Bulletin* **119**, 103–112.

ERİNÇ, S. 1955. Die morduologischen Entwicklungsstadien der Küçükmenderes Masse. *Review of the Geographical Institute of the University of Istanbul* **2**, 93–95.

GEMİCİ, Y., YILMAZER, Ç. & AKGÜN, F. 1992. Akçaşehir (Tire-İzmir) Neojen havzasının fosil makro ve mikroflorası [Macro and microfossil flora of the Akçaşehir (Tire-İzmir) Neogene basin]. *Turkish Journal of Botany* **16**, 383–393 [in Turkish with English abstract].

HAMILTON, J.W. & STRICKLAND, H.E. 1840. On the geology of the western party of Asia Minor. *Transactions of the Geological Society of London* **V-VI**, Second Series, 1–39.

JACKSON, J.A. & MCKENZIE, D.P. 1984. Active tectonics of the Alpine-Himalayan Belt between western Turkey and Pakistan. *Geophysical Journal of the Royal Astronomical Society* **77**, 185–264.

KAYA, T. 1987. Middle Miocene *Anchitherium* and *Aceratherium* Found in Tire (İzmir). *Journal of Faculty of Science Ege University* **B9**, 11–16.

KAYSERİ, M.S. & AKGÜN, F. 2008. Palynostratigraphic, palaeovegetational and palaeoclimatic investigations on the Miocene deposits in Central Anatolia (Çorum region and Sivas Basin). *Turkish Journal of Earth Sciences* **17**, 361–403.

KETİN, İ. 1968. Türkiye'nin genel tektonik durumu ile başlıca deprem bölgeleri arasındaki ilişkiler [Relations between general tectonic features and the main earthquake regions of Turkey]. *Mineral Research and Exploration of Turkey (MTA) Bulletin* **71**, 129–134. [in Turkish].

LIANG, M.M., BRUCH, A., COLLINSON, M., MOSBRUGGER, V., LI, C.S., SUN, Q. G. & HILTON, J. 2003. Testing the climatic estimates from different palaeobotanical methods: an example from the Middle Miocene Shanwang flora of China. *Palaeogeography, Palaeoclimatology, Palaeoecology* **198**, 279–301.

MCKENZIE, D.P. 1978. Active tectonics of the Alpine-Himalayan belt: the Aegean Sea and surrounding regions. *Geophysical Journal of Royal Astronomical Society* **55**, 217–254.

MOSBRUGGER, V., UTESCHER, T. & DILCHER, D.L. 2005. Cenozoic continental climatic evolution of Central Europe. *Proceedings of the National Academy of Sciences of the United States of America (PNAS)* **102(42)**, 14964–14969.

MOSBRUGGER, V. & UTESCHER, T. 1997. The coexistence approach – a method for quantitative reconstructions of Tertiary terrestrial paleoclimate data using the plant fossils. *Palaeogeography, Palaeoclimatology, Palaeoecology* **134**, 61–86.

NAKOMAN, E. 1971. Kömür [Coal]. *Mineral Research and Exploration of Turkey (MTA) Publication* **8**, Ankara [in Turkish].

OZANSOY, F. 1960. Ege Bölgesi karasal Senozoyik stratigrafisi (Balıkesir güneyi, Soma-Bergama, Akhisar-Manisa ve Kısmen Tire) [Cenozoic continental stratigraphy of Aegean region (southern Balıkesir, Soma-Bergama, Akhisar-Manisa and partly Tire)]. *Mineral Research and Exploration of Turkey (MTA) Bulletin* **55**, 1–27 [in Turkish with English abstract].

ÖZCAN, N. 1984. *Akçaşehir (Tire) Kuzeyinin Jeolojisi ve Paleontolojisi [Geology and Palaeontology of Northern Akçaşehir (Tire)]*. BSc Thesis. Dokuz Eylül Üniversitesi Mühendislik Fakültesi, [unpublished].

ÖZER, S., SÖZBİLİR, H., ÖZKAR, İ., TOKER, V. & SARI, B. 2001. Stratigraphy of Upper Cretaceous–Palaeogene sequences in the southern and eastern Menderes Massif (western Turkey). *International Journal of Earth Sciences* **89**, 852–866.

PHILLIPSON, A. 1910–1915. *Reisen und Forschungen im Westlichen Kleinasien*. Ergänzungshefte 167, 172, 177, 180, 183 der Petermanns Mitteilungen, Gotha, Jüstus Perthes.

PHILLIPSON, A. 1911. *Reisen und forschungen im Westlichen Klcinasien*. Petermanns Miu Erganzonpsheft, Gotha, 172.

PHILLIPPSON, A. 1918. *Kleinasien*. Handbuch der regionalen geologie **5**, 2.

ROJAY, B., TOPRAK, V., DEMİRCİ, C. & SÜZEN, L. 2001. Evolution of the Küçük Menderes graben (western Anatolia, Turkey). *Abstracts, Fourth International Turkish Geology Symposium*. Çukurova University, Adana, p. 23.

ROJAY, B., TOPRAK, V., DEMİRCİ, C. & SÜZEN, L. 2005. Plio–Quaternary evolution of the Küçük Menderes Graben Southwestern Anatolia, Turkey. *Geodinamica Acta* **18**, 317–331.

SANCAY, R.H., BATI, Z., IŞIK, U., KIRICI, S. & AKÇA N. 2006. Palynomorph, foraminifera, and calcareous nanoplankton biostratigraphy of Oligo–Miocene sediments in the Muş basin, Eastern Anatolia, Turkey. *Turkish Journal of Earth Sciences* **15**, 259–319.

SEYİTOĞLU, G. & IŞIK, V. 2009. Meaning of the Küçük Menderes graben in the tectonic framework of the central Menderes metamorphic core complex (western Turkey). *Geologica Acta* **7**, 323–331.

ŞENGÖR, A.M.C. 1982. Ege'nin neotektonik evrimini yöneten etkenler [Factors governing the neotectonic evolution of the Aegean]. *In*: EROL, O. & OYGÜR, V. (eds), *Batı Anadolu'nun Genç Tektoniği ve Volkanizması Paneli [Panel of Neotectonics and Volcanism of Western Anatolia]*. Congress of the Geological Society of Turkey, 59–72.

ŞENGÖR, A.M.C. 1987. Cross-faults and differential stretching of hanging walls in regions of low-angle normal faulting: examples from western Turkey. *In*: COWARD, M.P., DEWEY, J.F. & HANCOCK, P.L. (eds), *Continental Extensional Tectonics*. Geological Society, London, Special Publications **28**, 575–589.

ŞENGÖR, A.M.C., SATIR, M. & AKKÖK, R. 1984. Timing of tectonic events in the Menderes Massif, western Turkey: implications for tectonic evolution and evidence for Pan-African basement in Turkey. *Tectonics* **3**, 693–707.

ŞENGÖR, A.M.C., GÖRÜR, N. & ŞAROĞLU, F. 1985. Strike-slip faulting and related basin formation in zones of tectonic escape: Turkey as a case study. *In*: BIDDLE, K. & CHRISTIE-BLICK, N (eds), *Strike-slip Deformation, Basin Formation and Sedimentation*. Society of Economic Paleontologists and Mineralogists, Special Publication **37**, 227–264.

SÖZBİLİR, H. 2005. Oligo–Miocene extension in the Lycian Orogen: evidence from the Lycian molasse basin, SW Turkey. *Geodinamica Acta* **18**, 255–282.

TCHIHATCHEFF, P. DE. 1869. Asia Mineure (Description Physique) Quatrieme Partie Géologie*,* **III***,* Paris.

UNITED NATIONS 1974. *Mineral Exploration in Two Areas*. Technical Report 4, DP / DN / TUR–72 – 004/4, Turkey [unpublished].

ZACHOS, J., DICKENS, G. & ZEEBE, R. 2008. An early Cenozoic perspective on greenhouse warming and carbon-cycle dynamics. *Nature* **451**, 279–283.

ZACHOS, J., PAGANI, M., SLOAN, L., THOMAS, E. & BILLUPS, K. 2001. Trends, rhythms, and aberrations in Global Climate 65 Ma to Present. *Science* **292**, 686–693.

PLATE 1

Figures 1, 2, 3 & 6. Silty clayey laminated micritic carbonates (carbonate mudstone) (A) erosion surfaces, (B) bioturbation traces, (Q) quartz, (F) feldspar and (Mi) very thin mica flakes. 1–3: x10.6; 6: x27.5.

Figures 4, 5, 6 & 7. Silty and clayey fenestral pore bearing laminated microbial carbonates (microbial carbonate mudstone), Er– erosional surface, Ms– marble sand. 5: x10.5; 6: x5; 7: x10.5

Figure 6. Alternation of silty clayey laminated micritic carbonates (B) and silty and clayey fenestral pore bearing laminated microbial carbonates (B), (Er) erosional surface, (Bi) bioturbation. x27.5.

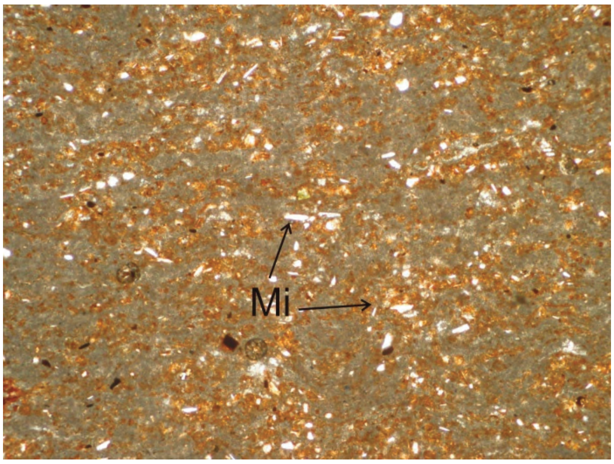

1 (ET-1)

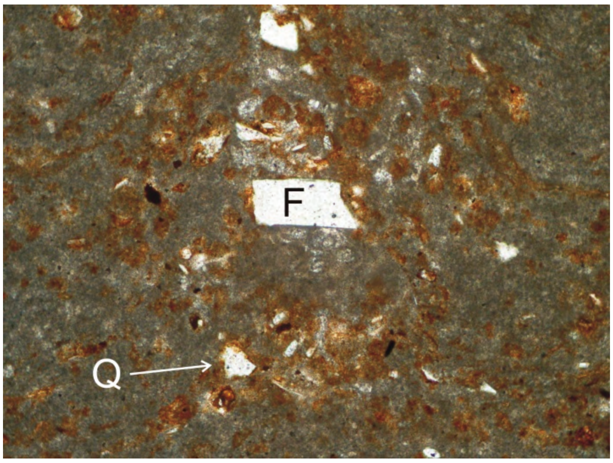

2 (ET-1)

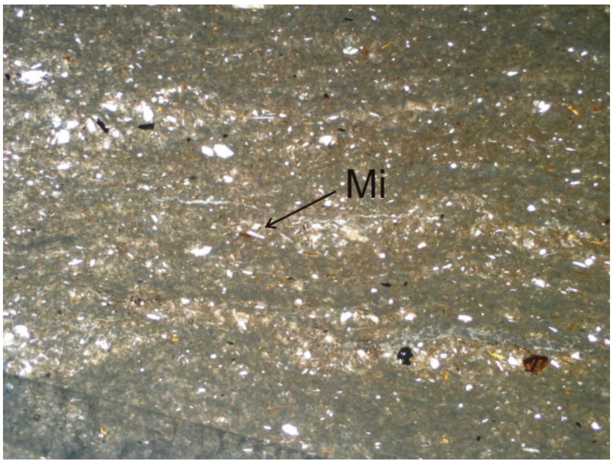

3 (ET-1)

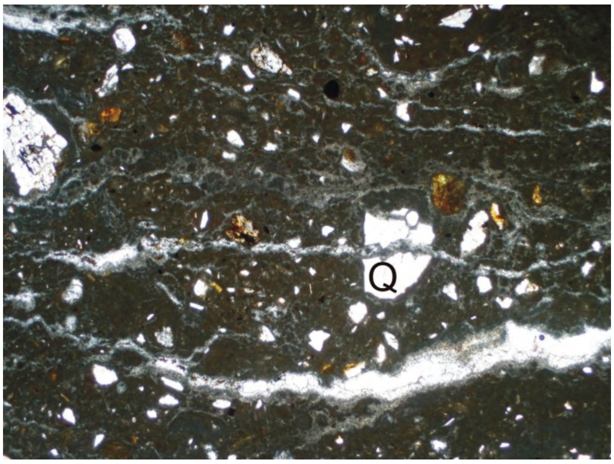

4 (ET-1)

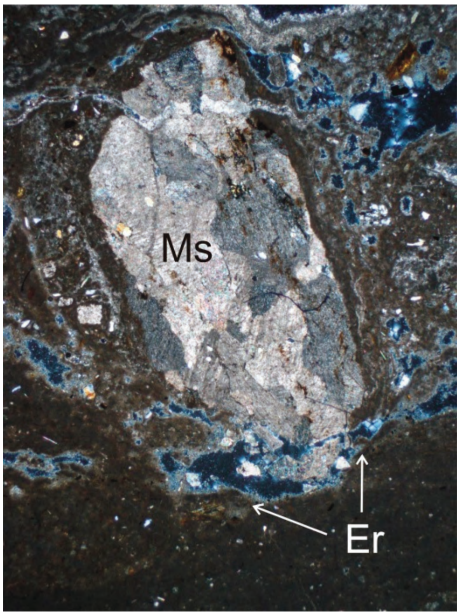

5 (ET-1)

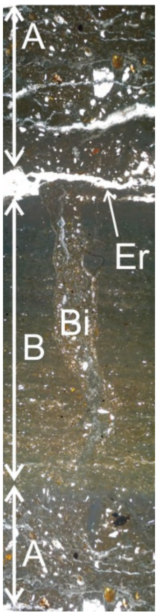

6 (ET-1)

7 (ET-1)

PLATE 2

Figures 1, 2, 3 & 4.	The pebbly calcarenitic sandstones, (Ms) marble sands, (Cc) pseudospar calcite cement, (Io) iron oxidized clay. x10.6.
Figure 5.	Silty and clayey, fenestral pore bearing laminated microbial carbonates (microbial carbonate mudstone), white arrows show shrinkage cracks. x10.6.
Figures 6, 7 & 8.	Bioturbated algal carbonate crust (bindstone), (Bi) bioturbation, (Rh) rhisolith. x10.6.

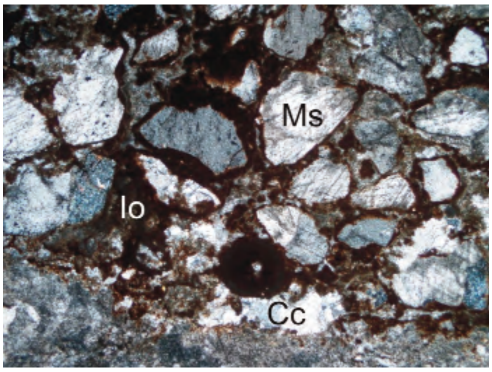

1 (ET-3)

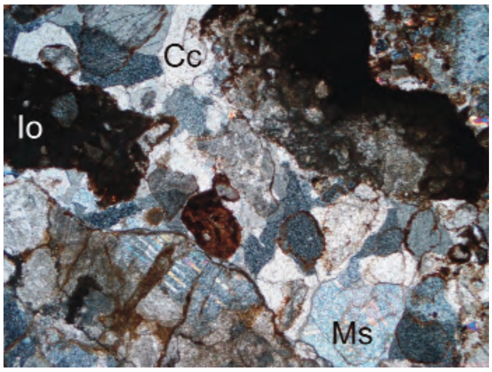

2 (ET-4)

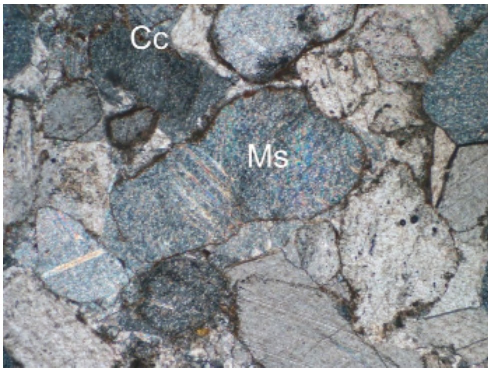

3 (ET-6)

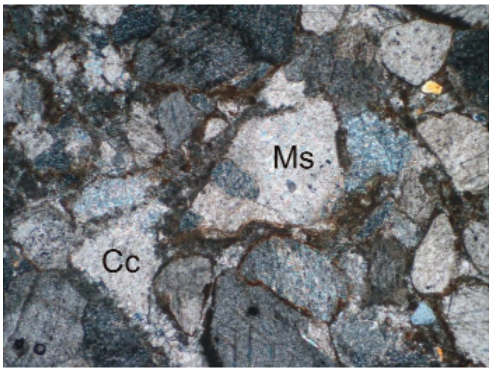

4 (ET-6)

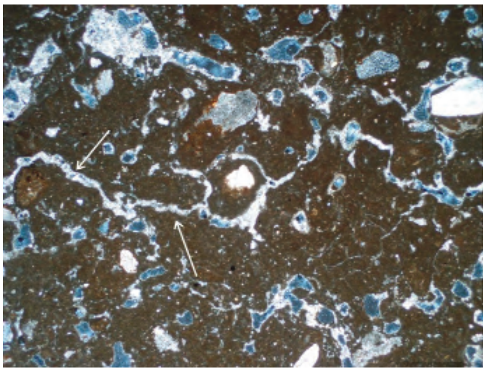
5 (ET-9)

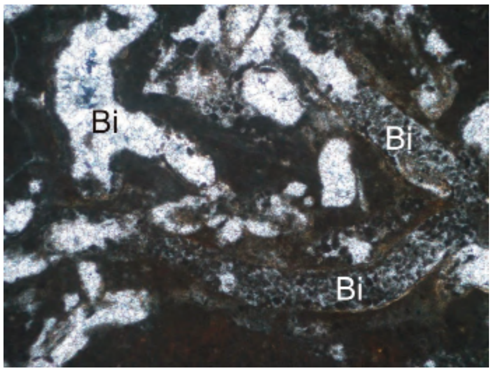

6 (ET-10)

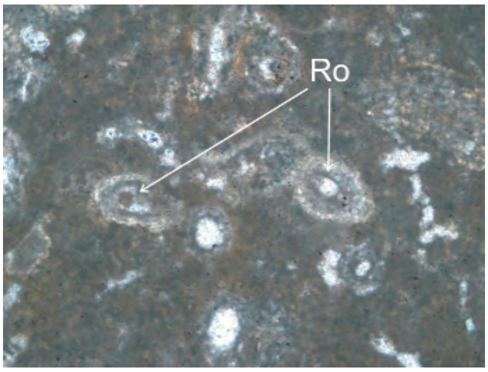

7 (ET-10)

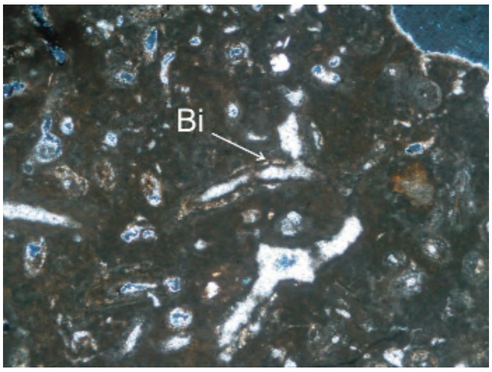

8 (ET-10)

PLATE 3

Figure 1.	Terrestrial and lacustrine carbonates (A) directly overlying basement rocks (B). x6.5.
Figures 2, 3 & 4.	Silty clayey laminated micritic carbonates (C), silty and clayey fenestral pore bearing laminated microbial carbonates (D) and bioturbated algal carbonate crust facies (E) constitute an alternating carbonate sequence. 2 and 4: x5.5; 3: x6.5.
Figures 5 & 6.	Pebbly-sandy, clayey micritic carbonates, (P) thin pebble, (S) sand and (Sl) silt sized metamorphic rock fragments. x10.6.

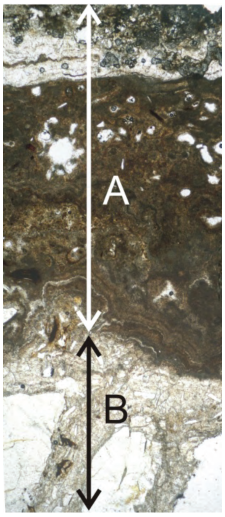

1 (ET-11B)

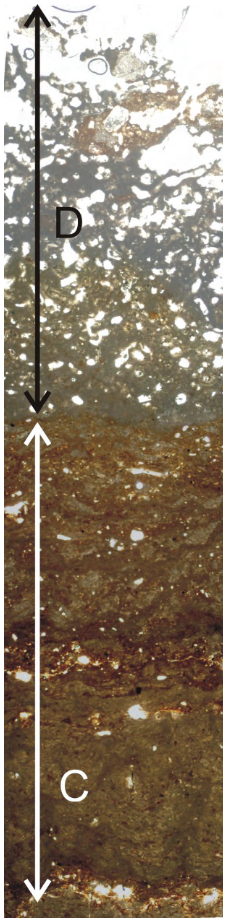

2 (ET-15A)

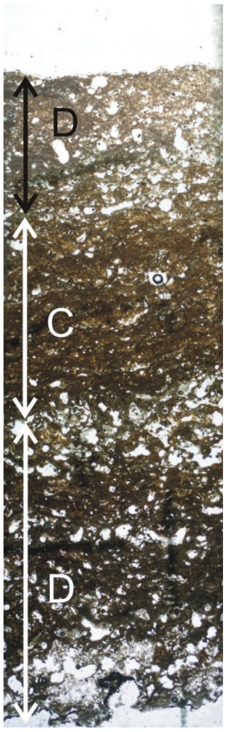

3 (ET-24)

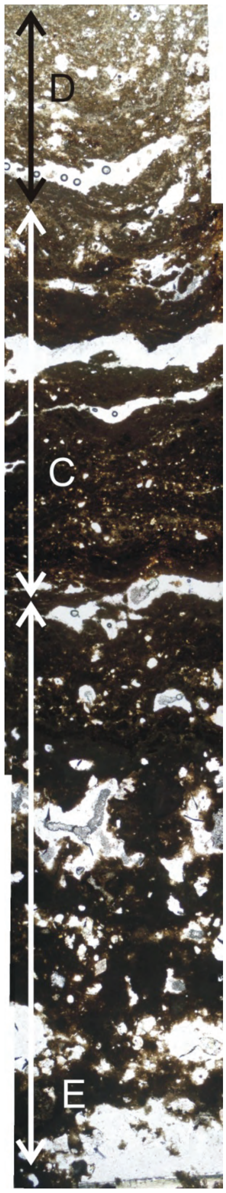

4 (ET-39)

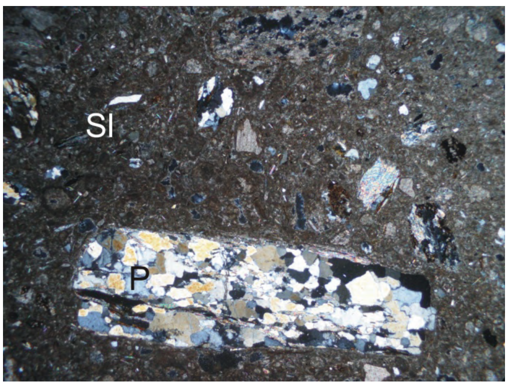

5 (ET-11A)

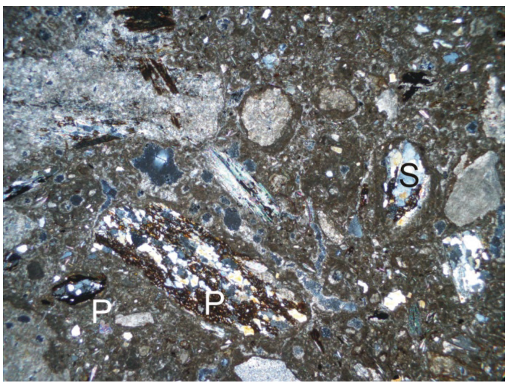

6 (ET-11A)

PLATE 4

Figures 1 & 2.	Bioturbated algal carbonate crust (bindstone). (Bi) bioturbation. 1-2: x10,6
Figures 3, 4 & 5.	Peloidal microbial carbonate (bindstone), algal peloidal micrite frame (mF) and spar calcite pore filling (Pf). 3–4: x10.6; 5: x21.
Figures 6 & 7.	Pebbly-sandy, clayey micritic carbonates (carbonate mudstone) (P) pebble, (S) sand sized metamorphic rock fragments. x10.6.
Figure 8.	Ostracod (Os) bearing microbial micritic carbonates (microbial carbonate mudstone). x10.6.

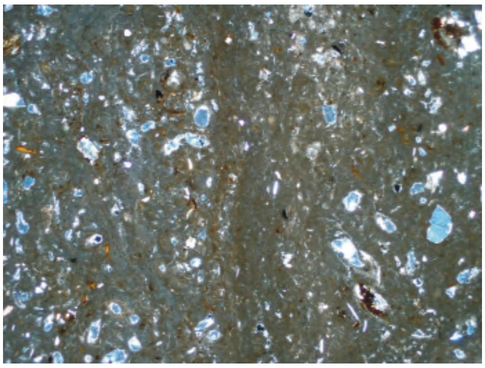

1 (ET-11A)

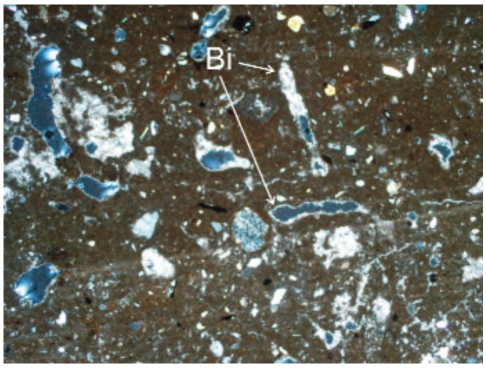

2 (ET-11A)

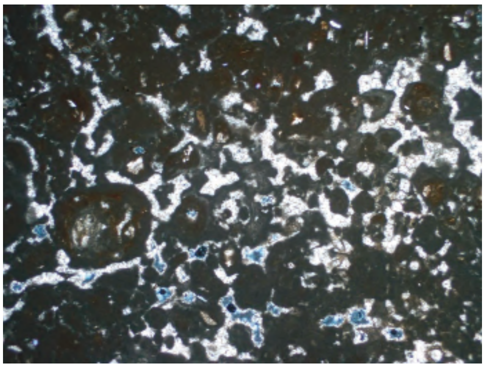

3 (ET-14)

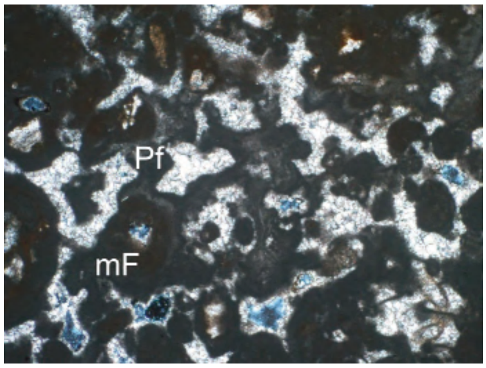

4 (ET-14)

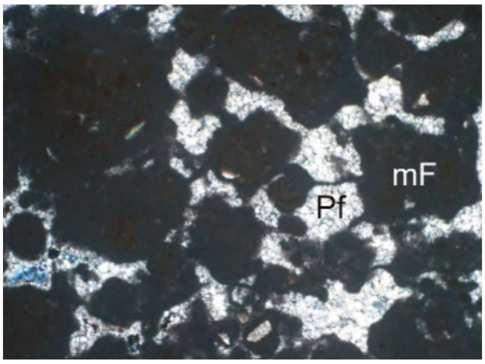

5 (ET-14)

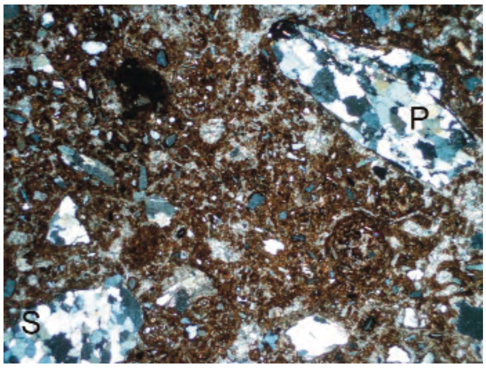

6 (ET-19)

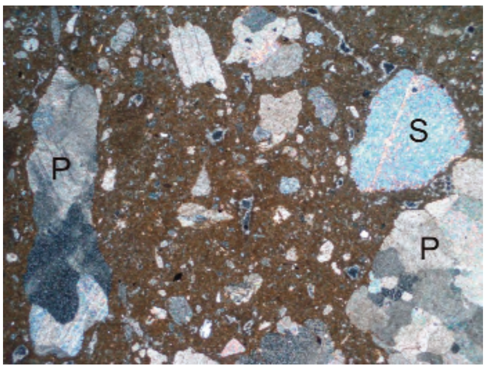

7 (ET-21)

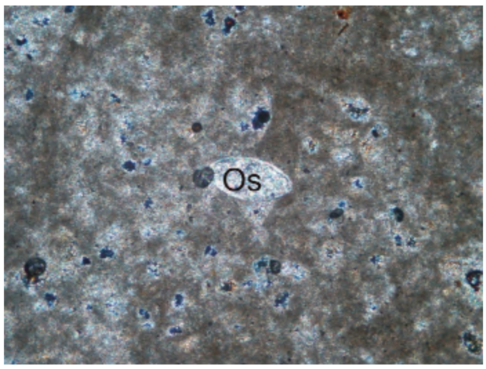

8 (ET-37)

PLATE 5

Figure 1. *Polypodiaceoisporites marxheimensis* (Mürriger & Pflug ex Thomson & Pflug) Krutzsch.
Figures 2 & 3. *Polypodiaceoisporites* sp.
Figure 4. *Laevigatosporites haardti* (Potonié & Venkatachala) Thomson & Pflug
Figure 5. *Pityosporites microalatus* (Potonié) Thomson & Pflug
Figure 6. *Podocarpidites libellus* (Potonié) Krutzsch
Figure 7. *Pityosporites* sp.
Figure 8. *Ephedripites* sp.
Figure 9. *Inaperturopollenites dubius* (Potonié & Venkatachala) Thomson & Pflug
Figure 10. *Cyacadopites* sp.
Figure 11. *Cupressacites insulipopillatus* (Trevisan) Krutzsch
Figure 12. *Sequoiapollenites polyformosus* Thiergart
Figures 13, 14 & 15. *Triatripollenites rurensis* Pflug & Thomson *in* Thomson & Pflug.
Figure 16. *Momipites punctatus* (Potonié) Nagy
Figures 17 & 18. *Subtriporopollenites simplex* (Potonié) Thomson & Pflug
Figure 19. *Tricolpopollenites henrici* (Potonié) Thomson & Pflug
Figure 20. *Tricolpopollenites microhenrici* (Potonié) Thomson & Pflug
Figure 21. *Tricolpopollenites densus* Pflug *in* Thomson & Pflug
Figure 22. *Tricolporopollenites cingulum* (Potonié) Thomson & Pflug ssp. *pusillus* (Potonié) Thomson & Pflug
Figure 23. *Cyrillaceaepollenites megaexactus* Potonié
Figures 24 & 25. *Periporopollenites* sp. (thallictrum type)
Figure 26. *Tetracolporopollenites* sp.

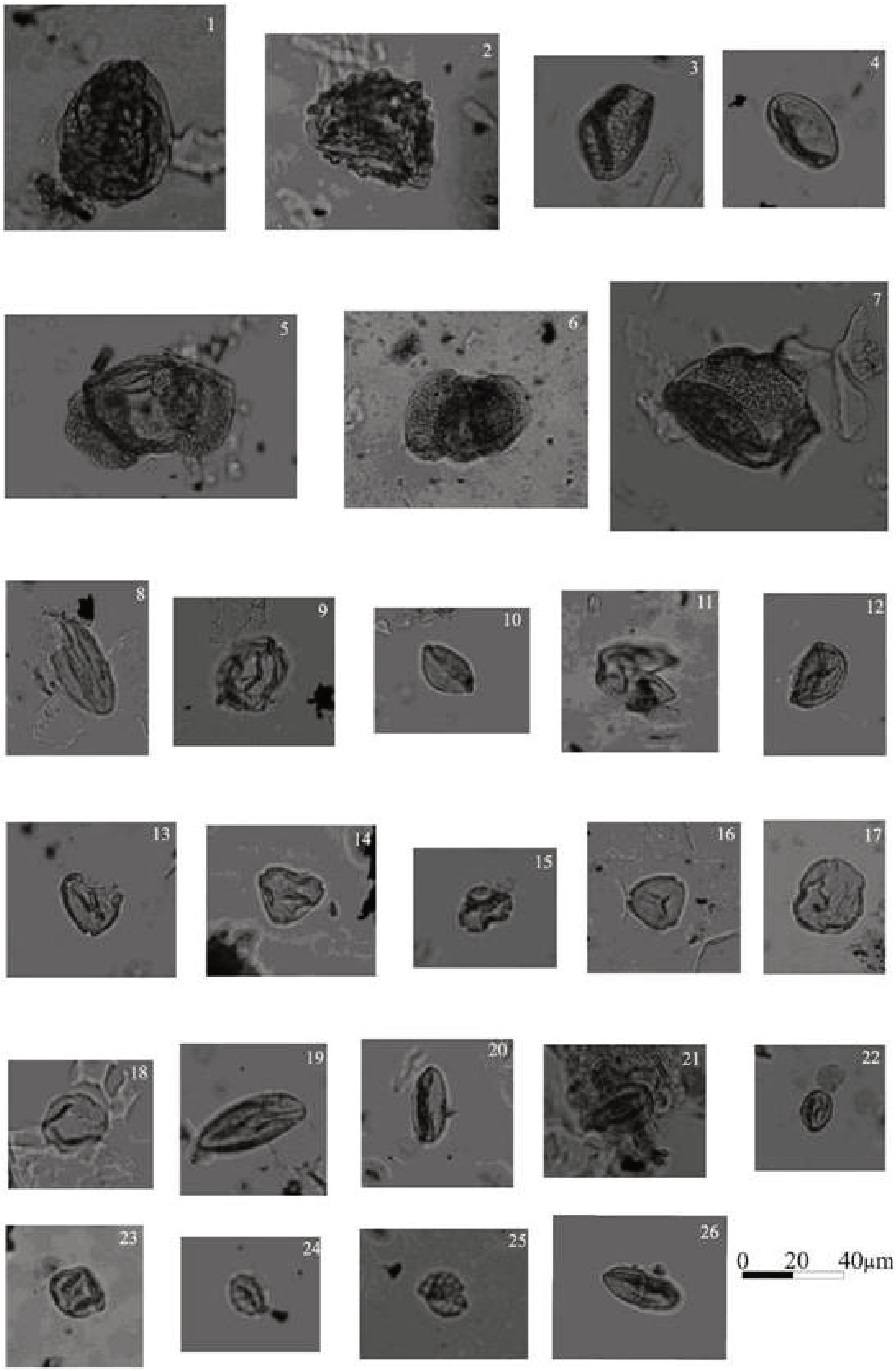
1
2
3
4
5
6
7
8
9
10
11
12
13
14
15
16
17
18
19
20
21
22
23
24
25
26
0 20 40μm